AD-A142 074 LOW-VOLTAGE MODEL STUDIES OF TRANSMISSION-LINE CONFIGURATIONS FOR PARTICL..(U) ARMY ARMAMENT RESEARCH AND DEVELOPMENT CENTER ABERDEEN PROVIN..

1/1

UNCLASSIFIED C E HOLLANDSWORTH MAY 84 ARBRL-TR-02560 F/G 20/7 NL

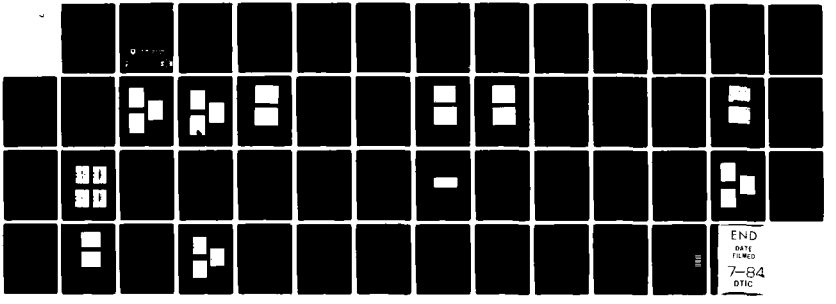

END

DATE FILMED

7-84

DTIC

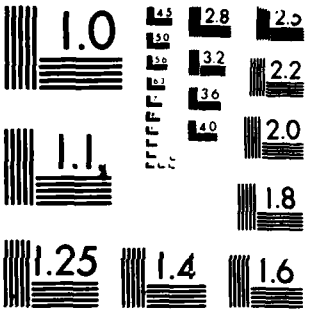

MICROCOPY RESOLUTION TEST CHART
NATIONAL BUREAU OF STANDARDS-1963-A

TECHNICAL REPORT ARBRL-TR-02560

LOW-VOLTAGE MODEL STUDIES OF TRANSMISSION-LINE CONFIGURATIONS FOR PARTICLE ACCELERATION

Clinton E. Hollandsworth

May 1984

US ARMY ARMAMENT RESEARCH AND DEVELOPMENT CENTER
BALLISTIC RESEARCH LABORATORY
ABERDEEN PROVING GROUND, MARYLAND

Destroy this report when it is no longer needed.
Do not return it to the originator.

Additional copies of this report may be obtained from the National Technical Information Service, U. S. Department of Commerce, Springfield, Virginia 22161.

The findings in this report are not to be construed as an official Department of the Army position, unless so designated by other authorized documents.

The use of trade names or manufacturers' names in this report does not constitute indorsement of any commercial product.

UNCLASSIFIED

SECURITY CLASSIFICATION OF THIS PAGE (When Data Entered)

REPORT DOCUMENTATION PAGE		READ INSTRUCTIONS BEFORE COMPLETING FORM
1. REPORT NUMBER TECHNICAL REPORT ARBRL-TR-02560	2. GOVT ACCESSION NO. ADA142074	3. RECIPIENT'S CATALOG NUMBER
4. TITLE (and Subtitle) LOW-VOLTAGE MODEL STUDIES OF TRANSMISSION-LINE CONFIGURATIONS FOR PARTICLE ACCELERATION		5. TYPE OF REPORT & PERIOD COVERED 6. PERFORMING ORG. REPORT NUMBER
7. AUTHOR(s) Clinton E. Hollandsworth		8. CONTRACT OR GRANT NUMBER(s)
9. PERFORMING ORGANIZATION NAME AND ADDRESS US Army Ballistic Research Laboratory, ARDC ATTN: DRSMC-BLB(A) Aberdeen Proving Ground, MD 21005		10. PROGRAM ELEMENT, PROJECT, TASK AREA & WORK UNIT NUMBERS RDT&E 1L16261AH80
11. CONTROLLING OFFICE NAME AND ADDRESS US Army AMCCOM, ARDC Ballistic Research Laboratory, ATTN: DRSMC-BLA-S(A) Aberdeen Proving Ground, MD 21005		12. REPORT DATE May 1984 13. NUMBER OF PAGES 49
14. MONITORING AGENCY NAME & ADDRESS (if different from Controlling Office)		15. SECURITY CLASS. (of this report) Unclassified 15a. DECLASSIFICATION/DOWNGRADING SCHEDULE

16. DISTRIBUTION STATEMENT (of this Report)

Approved for public release; distribution unlimited.

17. DISTRIBUTION STATEMENT (of the abstract entered in Block 20, if different from Report)

18. SUPPLEMENTARY NOTES

19. KEY WORDS (Continue on reverse side if necessary and identify by block number)

Accelerator
Linear Induction
Transmission-Line
Model Studies
Low-Voltage

20. ABSTRACT (Continue on reverse side if necessary and identify by block number) (idk)

Low-voltage model studies of various transmission-line configurations for particle acceleration have been carried out in parallel-plate and folded, coaxial cavity geometries as well as with coaxial cable arrays. To obtain some information on the waveform distortion caused by the line-junction discontinuities alone, ideal switches (avalanche transistors) were used to switch the charged lines. The analysis of Eccleshall and Temperley, for the general case of two-line systems and Eccleshall, for three-line (Continued on page 2)

DD FORM 1 JAN 73 1473 EDITION OF 1 NOV 65 IS OBSOLETE

UNCLASSIFIED

SECURITY CLASSIFICATION OF THIS PAGE (When Data Entered)

systems were verified in these experiments. For the case of impedance ratios which result in repetitive waveforms, these studies suggest that the effects of the line-junction discontinuities alone will not be severe enough to prohibit a limited number of beam passes when transmission-line cavities are used as the acceleration module in a recirculating linear-induction accelerator.

TABLE OF CONTENTS

LIST OF FIGURES

LIST OF FIGURES

I. INTRODUCTION

In recent years many applications that require the acceleration of intense currents ($\geq$ 1 kA) of relativistic electron beams (IREB) to energies well into the MeV range have emerged. Among these applications, two, weapons research and the radiography of transient phenomena wherein an IREB is used to produce a pulsed source of x-rays, are of special interest to the Ballistic Research Laboratory. The high currents and high particle energies required for these applications are difficult to achieve with pulsed diodes, electrostatic generators, RF linacs, or any of the various types of circular accelerators.

Single-stage IREB accelerators have been limited typically to energies of about 10 MeV. To achieve higher particle energies it is necessary to add energy in stages to the beam by having it pass through a succession of accelerating gaps (interspersed with drift or field-free regions) where the beam is subjected to a properly phased accelerating field. This multi-gap process is used, for example, in two well-known general types of accelerators, the RF linear accelerator and the linear induction accelerator (LIA).

In these machines the accelerating field is distributed along the entire length of the device, i.e., there is no single gap to which a voltage corresponding to the total acceleration voltage is applied. This feature provides an enormous practical advantage over single-stage accelerators: The final beam energy is raised simply by increasing the number of accelerating elements.

For currents in the kA range and larger an accelerator of the LIA class seems particularly appropriate. In these machines particles are accelerated across a gap on which a voltage is induced by a change in the magnetic flux contained within a circuit of which the beam is part. Leiss[1] has recently reviewed the state of development of accelerators based on the linear induction principle. He identifies two classes of linear induction accelerators as follows: (1) Core-type induction accelerators characterized by a constant cross sectional area and a time varying magnetic induction, and (2) line-type induction accelerators characterized by a constant magnetic induction and a changing cross-sectional area.

---

[1] *James E. Leiss, "Induction Linear Accelerators and Their Applications," IEEE Trans. Nucl. Sci. NS-26, No. 3, 3870-76, 1979.*

The technology of the core-type LIA has been developed at the Lawrence Livermore National Laboratory,[2-4] the Lawrence Berkeley Laboratory,[5] the National Bureau of Standards,[6] and at the Dubna Laboratory in the USSR.[7] The technology of the line-type induction accelerator, where the flux change results from moving electromagnetic waves in pulse lines or cavities, has received considerable attention in the USSR[8] and recently in the USA, at Sandia National Laboratory,[9,10] and at BRL.[11,12]

[2] *H. Christofilos, R.E. Hester, W.A.S. Lamb, D.D. Reagan, W.A. Sherwood, and R.E. Wright, "High Current Linear Induction Accelerator for Electrons," Rev. Sci. Instr. 35, 886-890, 1964.*

[3] *Ross E. Hester, Donald G. Bubp, John C. Clark, Alfred W. Chesterman, Edward G. Cook, Warren L. Dexter, Thomas J. Fessenden, Louis L. Reginato, Ted T. Yokota, and Andris A. Faltens, "The Experimental Test Accelerator (ETA)," IEEE Trans. Nucl. Sci. NS-26, No. 3, 4180-82, 1979.*

[4] *R.J. Briggs, D.L. Birx, G.J. Caporaso, T.J. Fessenden, R.E. Hester, R. Melendes, V.K. Neil, A.C. Paul, and K.W. Struve, "Beam Dynamics in the ETA and ATA 10 kA Linear Induction Accelerators: Observations and Issues," IEEE Trans. on Nuc. Sci. NS-28, No. 3, 3360-64, 1981. See also Physics Today, February 1982, p. 20.*

[5] *R. Avery, G. Behrsing, W.W. Chupp, A. Faltens, E.C. Hartwig, H.P. Hernandez, C. MacDonald, J.R. Meneghetti, R.J. Nemetz, W. Popenuck, W. Salsig and Vanecek "The ERA 4 MeV Injector," IEEE Trans. Nucl. Sci. NS-18, 479-483, 1971.*

[6] *J.E. Leiss, "Modern Electron Linacs and New User Needs," Proc. 1972 Proton Linac Conference, Los Alamos, LA-5115, UC-28 (1972).*

[7] *A.J. Anatskii, O.S. Boedanev, P.V. Bukaev, Yu P. Vakhrushin, I.F. Malyshev, G.A. Nalivaika, A.I. Pavlov, V.A. Suslov, and F.P. Khalchitskii, "Linear Induction Accelerator," Sov. At. En. 21, 1134-1140, 1966.*

[8] *A.I. Pavlovskii, V.S. Bosamykin, G.D. Kuleshov, A.I. Gerasimov, V.A. Tananakin, and A.P. Kumentev, "Multielement Accelerator Based on Radial Lines," Sov. Phys. Dokl, 20, 441-443, 1975.*

[9] *Radlac Radial Line Accelerator Progress Report, October 1977 Through 1978, Sandia National Laboratory Report, SAND-2129, Jan 1980.*

[10] *R.B. Miller, J.W. Poukey, B.G. Epstein, S.C. Shope, T.C. Genoni, M. Franz, B.B. Godrey, R.J. Adler and A. Mondelli, "Beam Transport Issues in High Current Linear Accelerators," IEEE Trans. Nucl. Sci., NS-28, No. 3, 3343-3345, 1981.*

[11] *D. Eccleshall and J.K. Temperley, "Transfer of Energy From Charged Transmission Lines With Application to Pulsed High-Current Accelerators," J. Appl. Phys. 49(7), 3649-3655, 1978. See also J.K. Temperley and D. Eccleshall, "Analysis of Transmission-Line Accelerator Concepts," USA ARRADCOM Technical Report, ARBRL-TR-02067, May 1978 (AD A056364), and J. K. Temperley, "Analysis of Coupling Region in Transmission-Line Accelerators," USA ARRADCOM Technical Report, ARBRL-TR-02120, Nov 1978 (AD A063463).*

[12] *D. Eccleshall, J.K. Temperley, and C.E. Hollandsworth, "Charged, Internally Switched Transmission Line Configurations for Electron Acceleration," IEEE Trans. Nucl. Sci., NS-26, No. 3, 4245 (1979).*

Eccleshall and Temperley (E/T) have presented a general analysis[11] of charged, constant-impedance, transmission-line pairs for particle acceleration. In the E/T schemes the required switches are located inside the charged cavities. Independently Smith[13] has analyzed pulse-line accelerator structures in which the energy is stored (and switched) external to the cavity.

The main thrust of the E/T effort has been to identify cavity structures which are highly efficient in transferring stored energy from the cavity structure to a pulsed electron beam and which also offer voltage gain and the potential for large acceleration gradients. The properties of the induction voltage or acceleration waveform, e.g., pulse durations and pulse amplitudes, can be parameterized in terms of the impedance ratio of the line pairs and the charge voltage. For the general problem of arbitrary impedance ratios and ideal lossless lines, Eccleshall and Temperley determined the conditions for maximum efficiency and maximum transfer of stored energy from the cavity to a resistive beam load.

Examples of the type of line-pairs appropriate to the E/T analysis are given in Figs. 1(a) and 1(b). In Fig. 1(c) the equivalent circuit for these asymmetric (unequal but uniform impedance) line pairs, or any pair of uniform transmission lines, is given. The equivalent circuit generators set up the initial condition, i.e., the generator in Line 1 generates a voltage step $-V_0$, the charge voltage, at $\tau = 0$, and the generator in Line 2 applies a voltage V_0 across the (open circuit) output at $\tau = 0$.

The region of the junction between lines 1 and 2 is a region of discontinuity, i.e., it is not possible to match fields on both sides of the discontinuity, using waves in the principal, (transmission-line) mode only. Higher order modes must be introduced in order to satisfy Maxwell's equation and the appropriate boundary conditions.

Whinnery et. al.[14-16] described the discontinuities of Fig. 1 by introducing an equivalent circuit located between the two lines and calculated equivalent circuit parameters for several different geometries. Recently Sidel[17] has found inconsistencies in the method employed by Whinnery et. al. and presented an alternative solution to the problem. He finds that, while the difference between the two solutions may be negligible for slow risetime pulses, they become increasingly significant for faster risetime pulses, large physical dimensions, or slow velocity in the line. These differences are not expected to be prominent in the present experiments.

[13] *Ian D. Smith, "Linear Induction Accelerators Made From Pulse-Line Cavities With External Pulse Injection," Rev. Sci. Instrum. 50, 714, 1979.*

[14] *J.R. Whinnery and H.W. Jamieson, "Equivalent Circuits for Discontinuities in Transmission Lines," Proc. IRE 32, 98-115, 1944.*

[15] *J.R. Whinnery, H.W. Jamieson and T. E. Robbins, "Coaxial-Line Discontinuities," Proc. IRE 32, 695-704, 1944.*

[16] *J.R. Whinnery and D.C. Stinson, "Radial Line Discontinuity," Proc. IRE 43, 46-51, (1955).*

[17] *David B. Sidel, "Discontinuity Effects on Radial Cavity Transmission Lines," Sandia Laboratories Report SAND-79-1056, April 1979.*

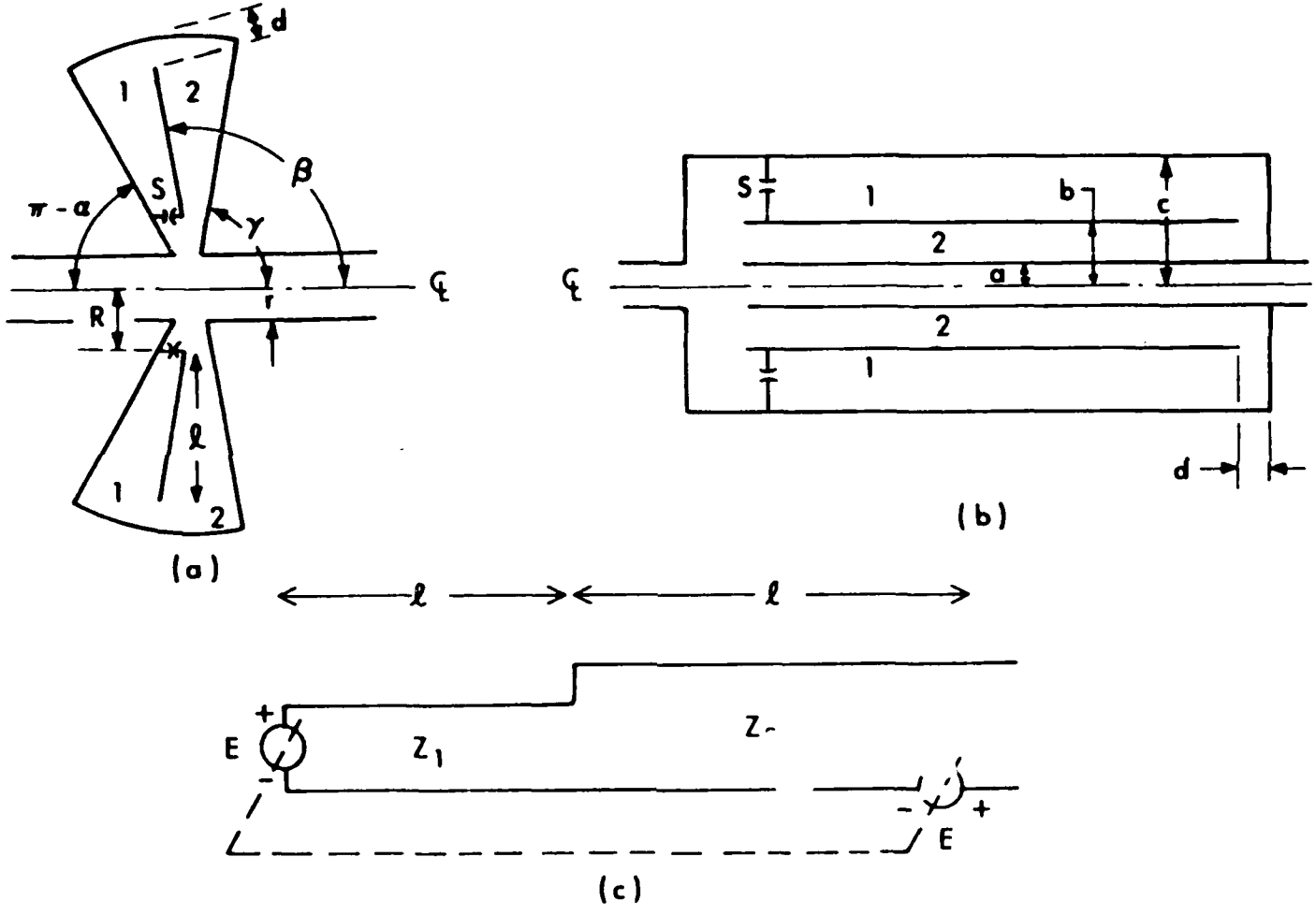

Figure 1. Transmission-Line Cavity Geometries. (a) Asymmetric radial line, (b) asymmetric coaxial line, (c) equivalent circuit for asymmetric line cavities. We shall refer to d as the discontinuity length.

Experimental investigations are described in this report which were initiated in order to study, under ideal conditions, the effects of the line-junction region on the open circuit output of the cavities as well as to verify the E/T analysis (Eccleshall and Temperley ignored the effects of the junctions in their initial analysis). The simple low-voltage models adopted in the work permit rapid parameter changes and may be more appropriate than computational studies when it is desired to follow pulse propagation through many traversals of the cavity structure.

During the course of these experimental studies on two-line systems the analysis of three-line pulse-line cavities, originally reported by E/T[11] and Smith,[13] was continued. This analysis[18] identified a class of three line systems analogous to the two-line system and a preliminary summary of the three-line analysis, and some related experimental work has already been given.[19] In the following sections of this report we discuss, separately, experiments on models of two- and three-line systems.

II. EXPERIMENTAL (TWO-LINE SYSTEMS)

The open-circuit waveform for arbitrary impedance from the line-pair shown in Fig. 1 is a sequence of steps given by Eccleshall and Temperley as

$$V^{(m)} = (-1)^m \frac{\sin\left(\frac{2m+1}{2}\right)x}{\sin\frac{x}{2}}, \quad x = \arccos \rho \tag{1}$$

where $V^{(m)}$ is the mth step of duration $2T_1$, the double transit time of the line. The quantity ρ is the reflection coefficient for a wave traveling from line 1 to line 2.

$$\rho = (Z_2 - Z_1)/(Z_2+Z_1) \quad , \tag{2}$$

where Z_1, Z_2 are the characteristic impedances of the lines.

One of the more interesting and important results of the E/T analysis is the prediction that the open circuit (OC) voltage for certain impedance ratios is repetitive. In equation (1) if $x = \frac{p}{q}\pi$, p and q integers with no common factors, the voltage is a repetitive pattern with period $2qT_1$ if p and q are both odd and period $4qT_1$ if either p or q is even. This result facilitates confirmation of the E/T analysis because the periods for the first few cases of interest are short enough that a few cycles of the waveform may be observed before appreciable attenuation of the signal in the test cavity complicates the interpretation of the waveform.

---

[18] I. Eccleshall, private communication.

[19] Ian Eccleshall and J.E. Hollingsworth, "Transmission-Line Cavity Linear-Induction Accelerator," IEEE Trans. Nucl. Sci. NS-28, No. 3, 3286 (1981).

A. Cable Experiments

The waveforms predicted by the Eccleshall-Temperley analysis are easily demonstrated with a mercury switch and pairs of coaxial-cable arrays, each array consisting of cables in parallel as required to achieve the desired impedance ratios. In the present equipment equal lengths of RG-174/U 50 Ω cable were used with the center conductors connected to a low-voltage power supply through a 35 K Ω charging resistor. A mercury switch operated at a few hundred Hz shorted the center conductor to ground at one end of the array; the open-circuit voltage was observed at the opposite end of the array with a high input-impedance oscilloscope.

Figures 2 and 3 show the predicted and observed waveforms for three impedance ratios which, according to Eq. (1), produce repetitive waveforms, $Z_2/Z_1 = 1$, 3 and 1/3, respectively. Further confirmation of the repetitive nature of the waveform is shown in Fig. 4. Pulse deterioration due to losses in the line are evident on this compressed time scale but that the pattern is a recurring one is obvious. The $Z_2/Z_1 = 1$, $\rho = 0$, case was identified by Pavlovskii and, in the biconic line configuration of Fig. 1(a), was used in the basic acceleration cell of the first pulse-line accelerator, which was built by Pavlovskii and collaborators.

The packaging of the mercury switch includes a short section of 50 Ω line which is always interposed between the switched end of the coaxial arrays and the switch element itself. This results in an L/R time constant which produces a noticeable effect on the waveform when a low impedance line is switched: e.g., Fig. 3(b) where $Z_1 = 16.7$ Ω and $Z_2 = 50$ Ω.

Figure 5 shows oscilloscope traces obtained for $Z_2/Z_1 = 1/4$. This ratio does not satisfy the requirements for periodicity but is rather close to a ratio which does ($Z_2/Z_1 = 1/4.30$ produces a recurring waveform). The waveforms are very similar for the two cases. If one imagines a line pair with this impedance ratio in a practical solution, i.e., where a coupling region which produces risetime deterioration exists, the abrupt changes of Fig. 5 would be smoothed out after a few transversals of the line and the overall appearance would approximate a decaying sine wave. Such a wave is potentially attractive in terms of a recirculating-beam concept which has the potential for achieving high acceleration gradients. However, such ratios are difficult to achieve in most practical geometries.

Because Eccleshall and Temperley assumed ideal switches and ignored the line junctions, the cable experiments provide an appropriate simulation for verification of their analysis. Although discontinuities exist at the point where the cable arrays are joined together, the important parameters, transverse dimension, wavelength, etc., are such that the e-folding length for attenuation of the higher order modes should be very short, and the effect of the discontinuity insignificant.

B. Parallel-Plate Transmission Line Experiments

The cable experiments described in the preceding section, while they verify analysis, are not totally representative of real devices which are

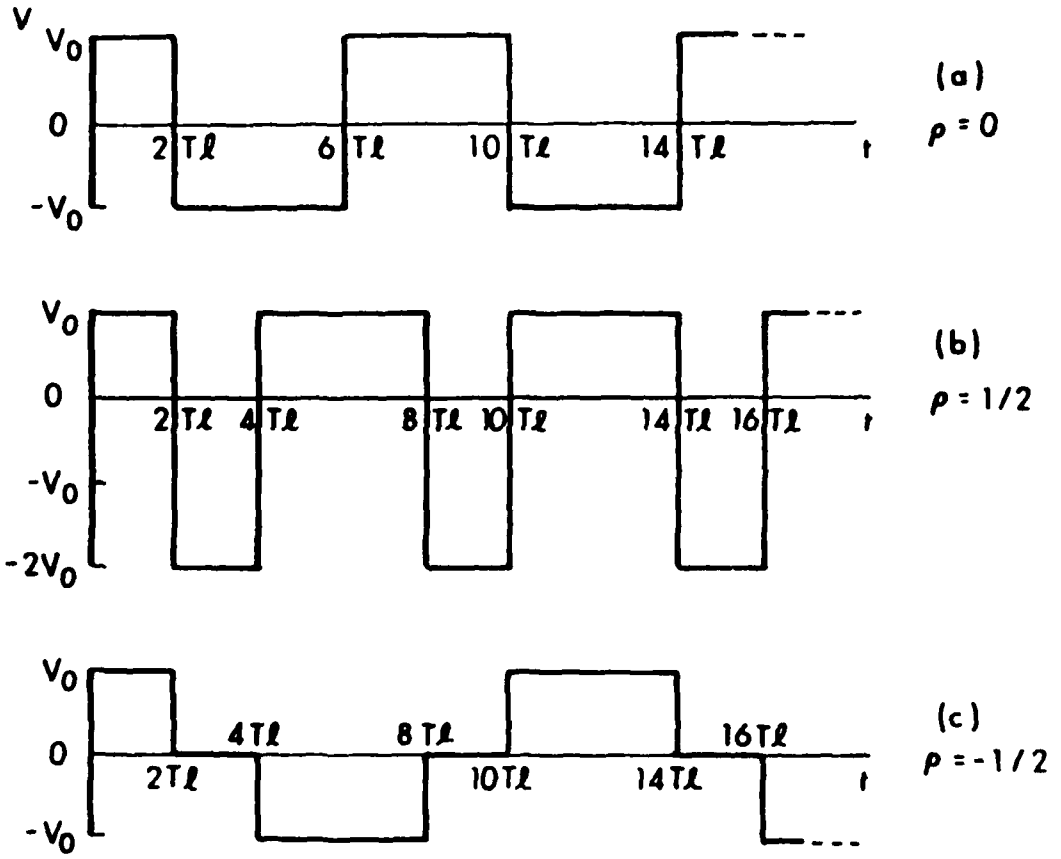

Figure 2. Open-Circuit Output Voltages for Several Line-Impedance Pairs. (a) $Z_2 = Z_1$. (b) $Z_2 = 3Z_1$. (c) $Z_2 = Z_1/3$.

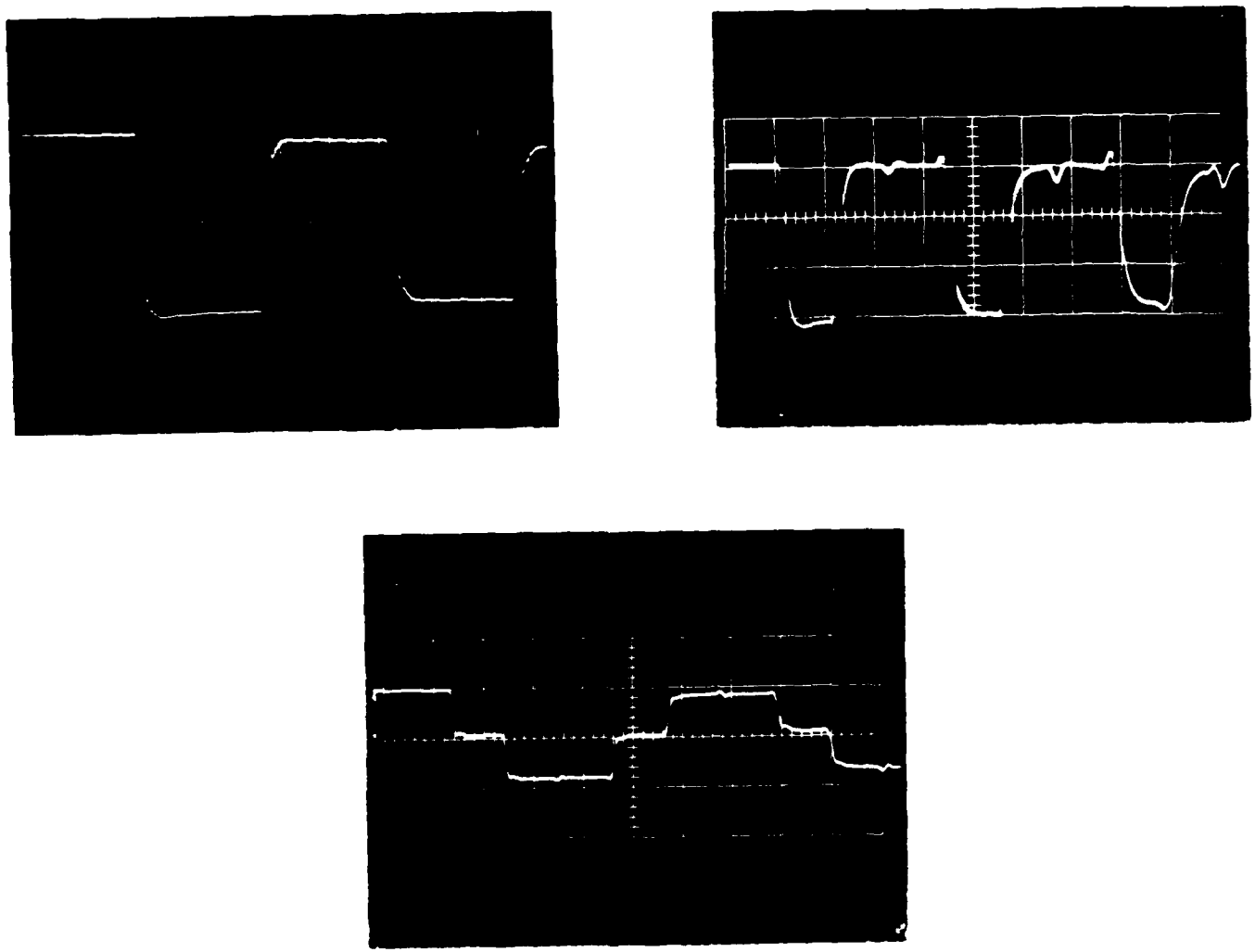

Figure 3. Open-Circuit Waveforms From Coaxial-Cable Arrays. Time calibration is approximately 50 ns/div. (a) $Z_2 = Z_1$. (b) $Z_2 = 3Z_1$. (c) $Z_2 = Z_1/3$.

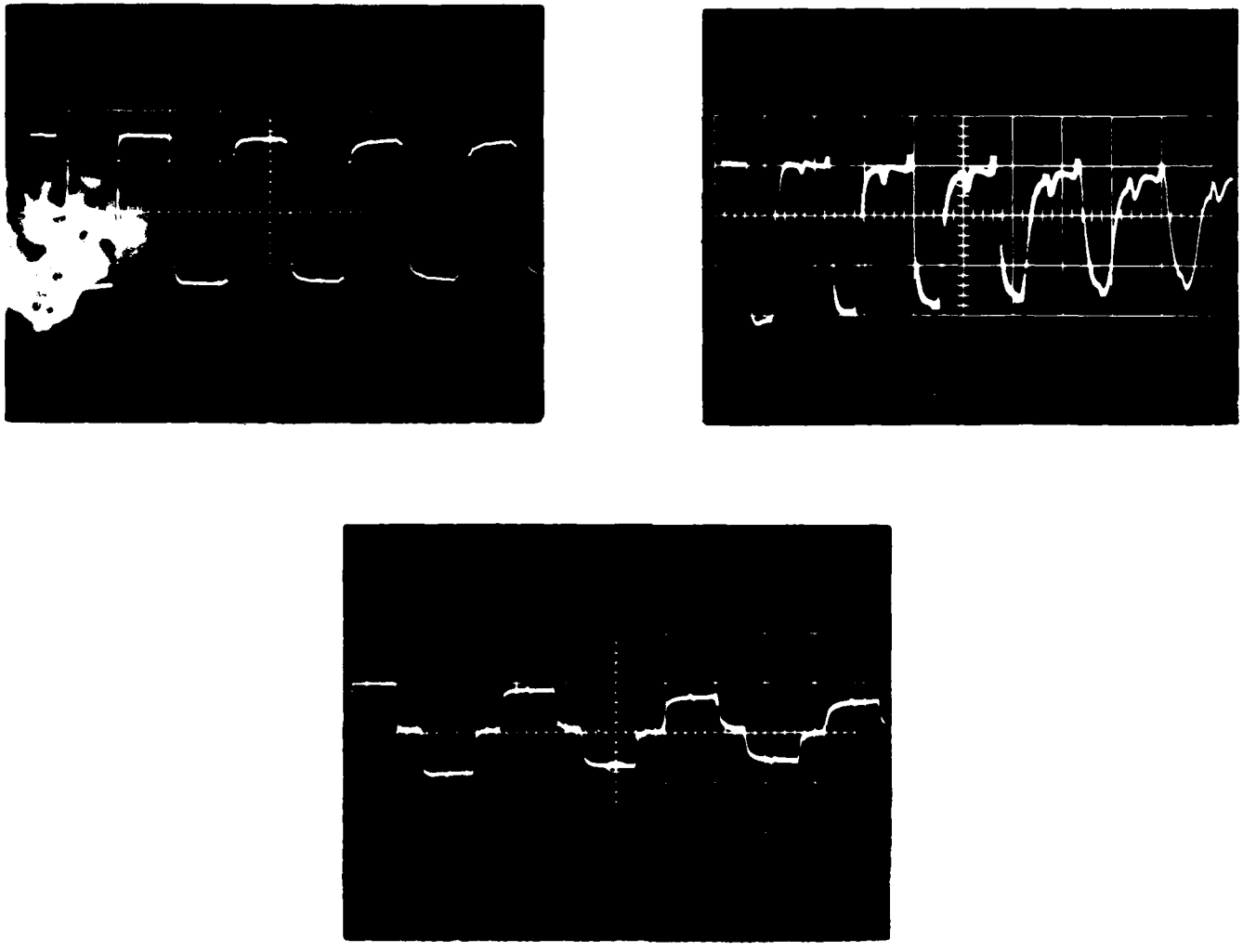

Figure 4. Open-Circuit Waveforms From Coaxial-Cable Arrays. Time scale is uncalibrated. (a) $Z_2 = Z_1$. (b) $z_2 = 3Z_1$. (c) $Z_2 = Z_1/3$.

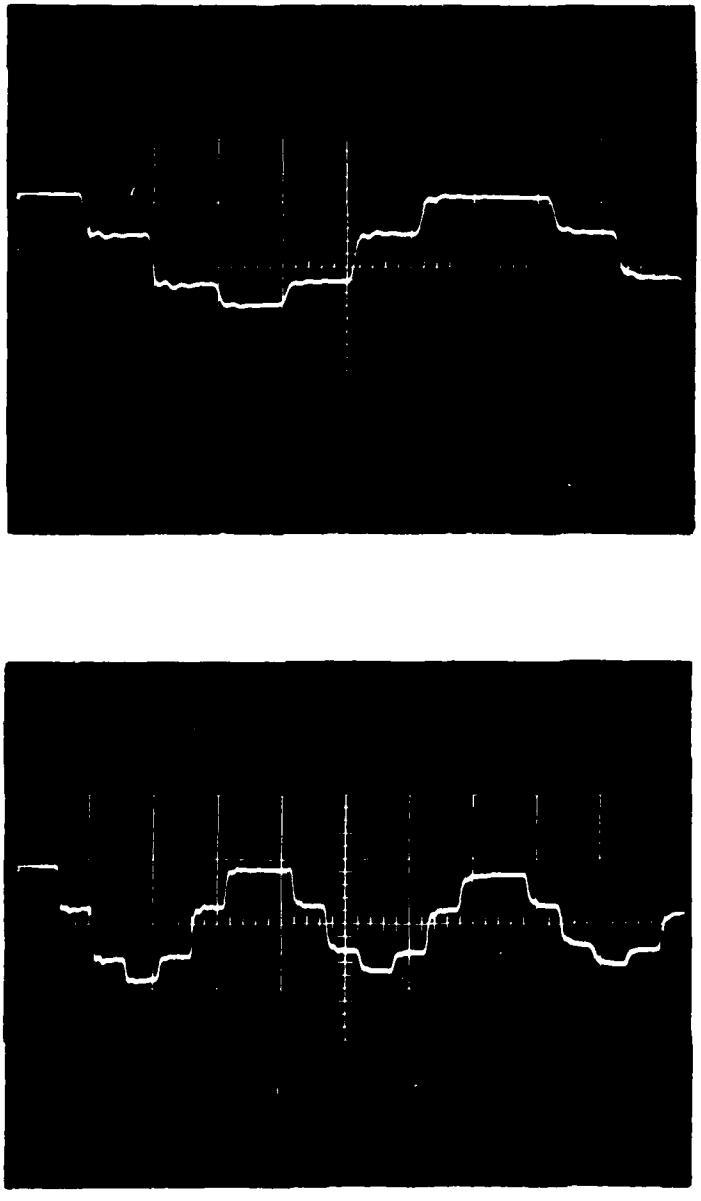

Figure 5. Open-Circuit Voltage for $Z_2 = 1/4Z_1$ Array. Time calibrations are approximately 50 ns/div for (a) and 100 ns/div for (b).

likely to be closed cavity structures (similar to those depicted in Fig. 1) filled with a liquid dielectric. Voltage standoff requirements may lead to rather large discontinuity regions in some geometries. To obtain some indication of the problems to be encountered in a real device, experiments were initiated in a parallel-plate geometry which offers the particular advantages of simple and inexpensive fabrication and considerable flexibility.

In the course of these experiments two different line pairs were used: (1) a 3.05 M long assembly made of circuit-board material and (2) a 1.83 M long line fabricated from sheet metal. Figure 6 shows the geometries. Because the fields extend beyond the conductor boundaries in this geometry the middle, or ground plane, conductors in Fig. 6 were made double the width of the outer conductors in order to minimize crosstalk between the two lines. The outer conductor widths were 15.2 cm for the circuit-board unit and 30.5 cm for the sheet-metal model. Uniformity of plate spacings was maintained by lucite spacers in conjunction with nylon rods.

Switching was accomplished by avalanche transistor circuits with switching times of less than one nanosecond. The switches were operated at a repetition rate of approximately one kHz. Output signals were derived from a sensor capacitor (C in Fig. 6). This capacitor had dimensions of 10.16 cm by 2.54 cm (in the direction of wave propagation) and a plate separation of approximately 5×10^{-3} cm with a mylar dielectric. A sampling oscilloscope was used to record the open-circuit voltage waveforms in a storage mode.

A major difficulty in the experiments with parallel-plate systems is that the ratio of the sensor signal V_s to the actual voltage between the plates is $(V_s/V_0) \approx 10^{-4}$. Since the transmission-line field is not enclosed by conducting surfaces its strength outside the plates can be orders of magnitude larger than the sensor signal. Thus coaxial cables with solid outer conductors, semirigid 50 Ω cable, were used to transmit the sensor signal to an oscilloscope.

Figure 7(a) shows the output for a $Z_2 = Z_1 = 47\ \Omega$, 3.05 M line and for two extreme examples of discontinuity length, d in Fig. 1(a), which are much larger and much smaller than the parallel plate spacing, h. The longer risetimes and more rapid deterioration in overall quality of the pulse in the large discontinuity configuration are evident. In practice the discontinuity, d, need only be large enough to satisfy voltage standoff requirements, i.e., $d \approx h$, the smallest line spacings. The output signals were derived from the capacitive pickoff and the associated RC time constant at the output is responsible for the decaying exponential component of the pulse train envelope.

More detail on risetime deterioration is provided in Fig. 7(b). The superimposed traces are the same as in Fig. 7(a). The upper and lower traces show the regions around $\tau = 2T\ell$ and $\tau = 6T\ell$, respectively. This figure shows that the basic character of the waveform is not appreciably changed by many transversals of the discontinuity between the line pairs.

A particularly promising line pair for electron acceleration, hereafter referred to as E/T-1, is that pair defined by $Z_2/Z_1 = 3$. For a matched load and charging voltage V_0, this configuration gives an accelerating voltage of

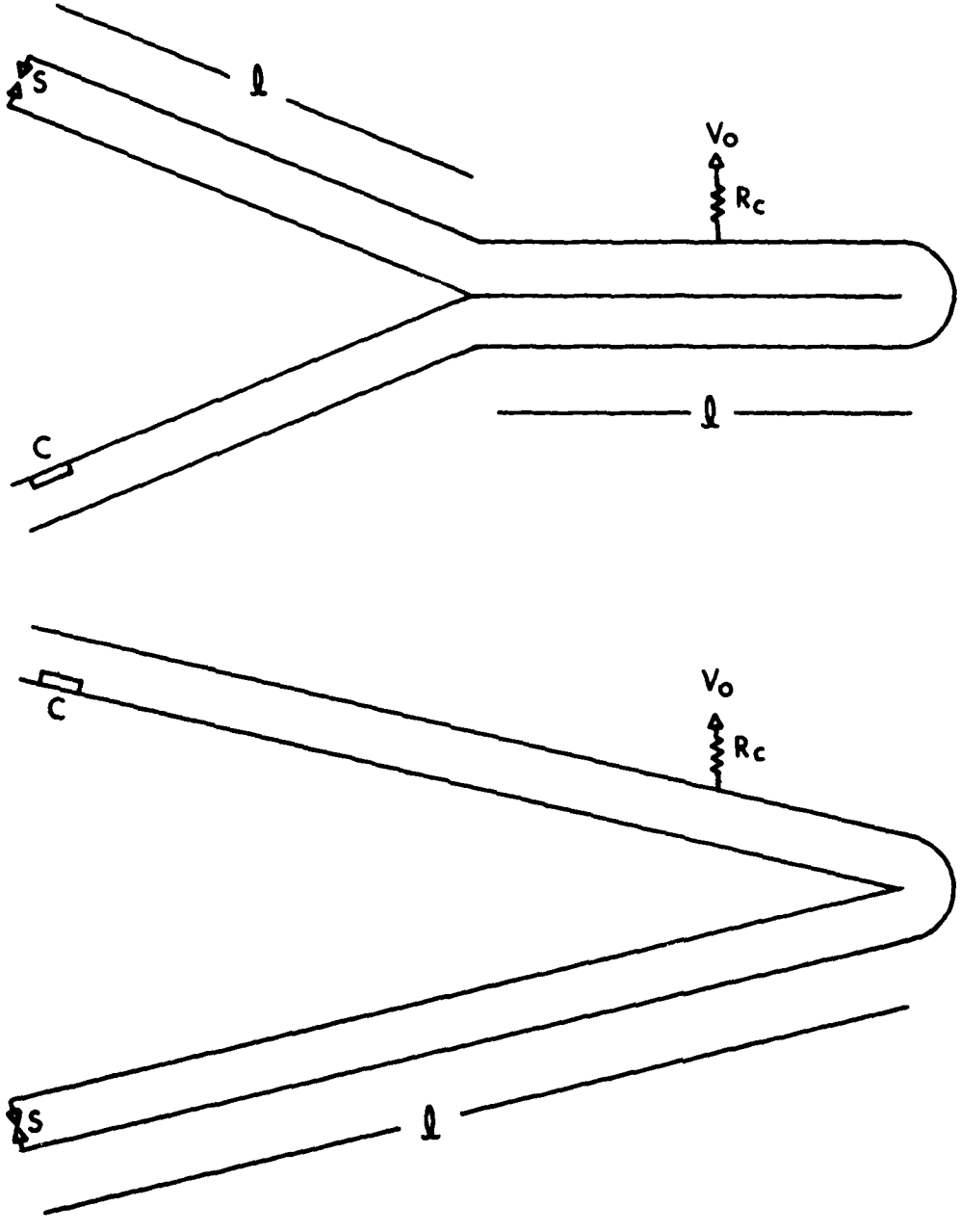

Figure 6. Line Drawings of Parallel-Plate Transmission Lines. (a) Circuit-Board Array. (b) Sheet Metal Array. S denotes location at switch array (one to five used), C is the Sensor Capacitor (not to scale) and V_0 and R_c represent the charge voltage and charging resistance respectively.

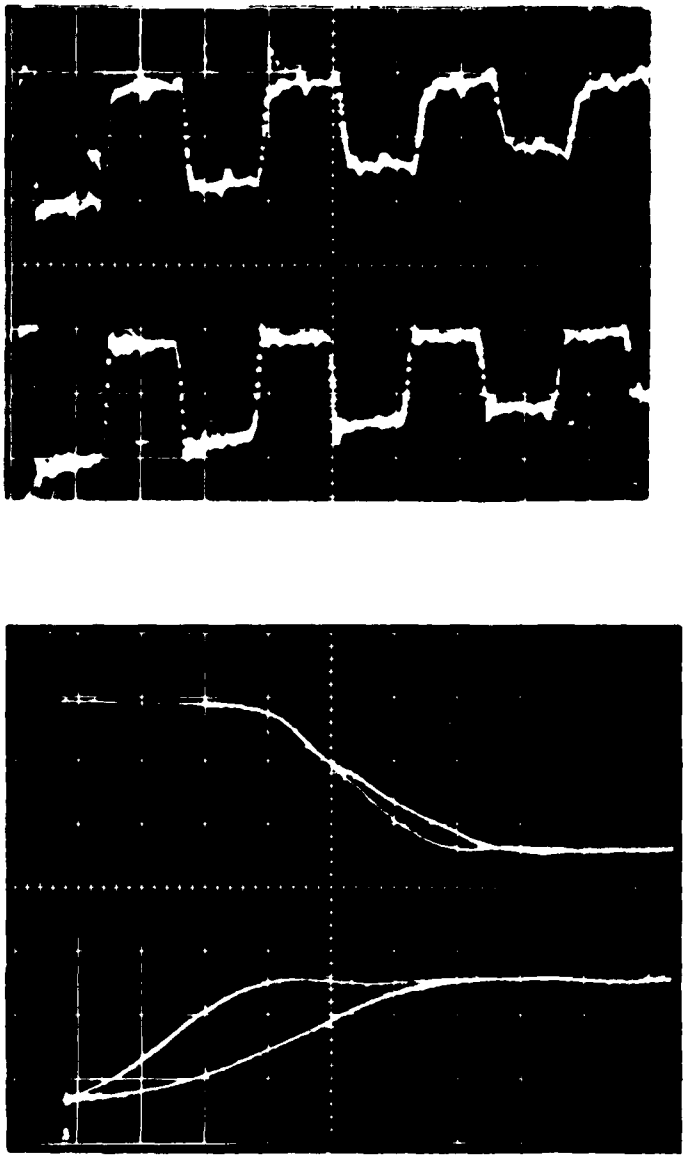

Figure 7. Open-Circuit Voltage for 47Ω ($Z_1 = Z_2$) Parallel-Plate Line ($2T\ell$ = 20 ns). (a) Time/div uncalibrated. (b) Time/div = 1 ns. Top waveform in (a) has d/h = 6 while for bottom photo the ratio d/h = 0.38.

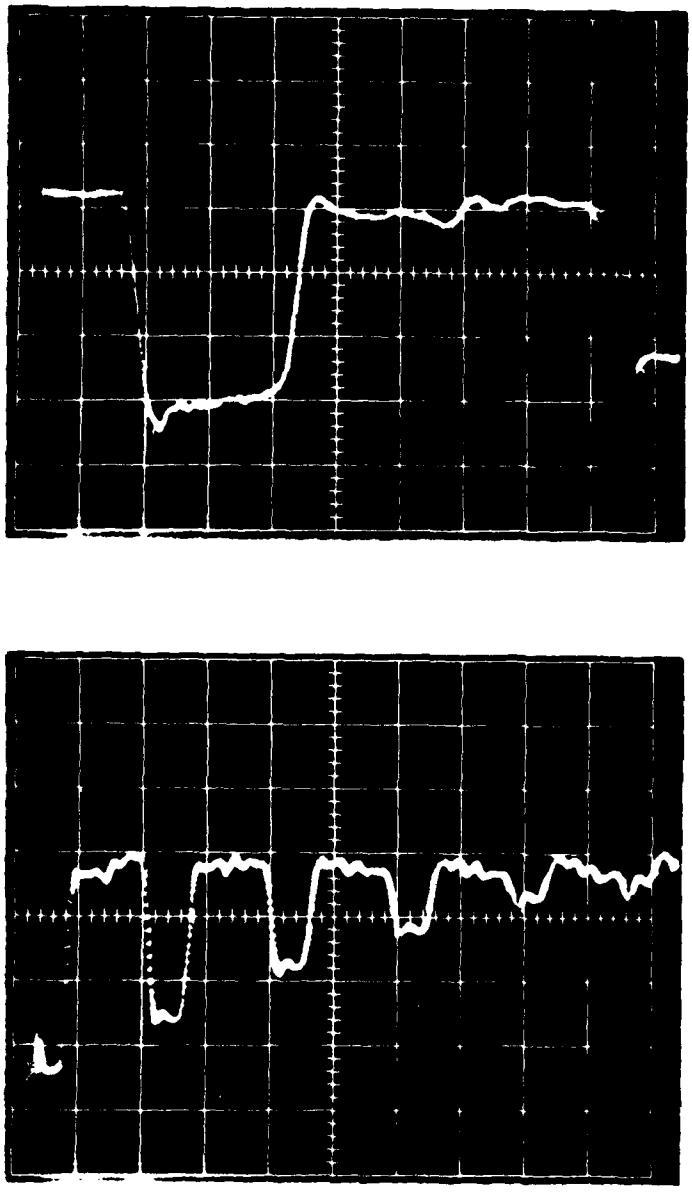

Figure 8. Output Waveform for $Z_2 = 3Z_1$ with Sheet-Metal Line-Pair.
(a) 5 ns/div. (b) 20 ns/div.

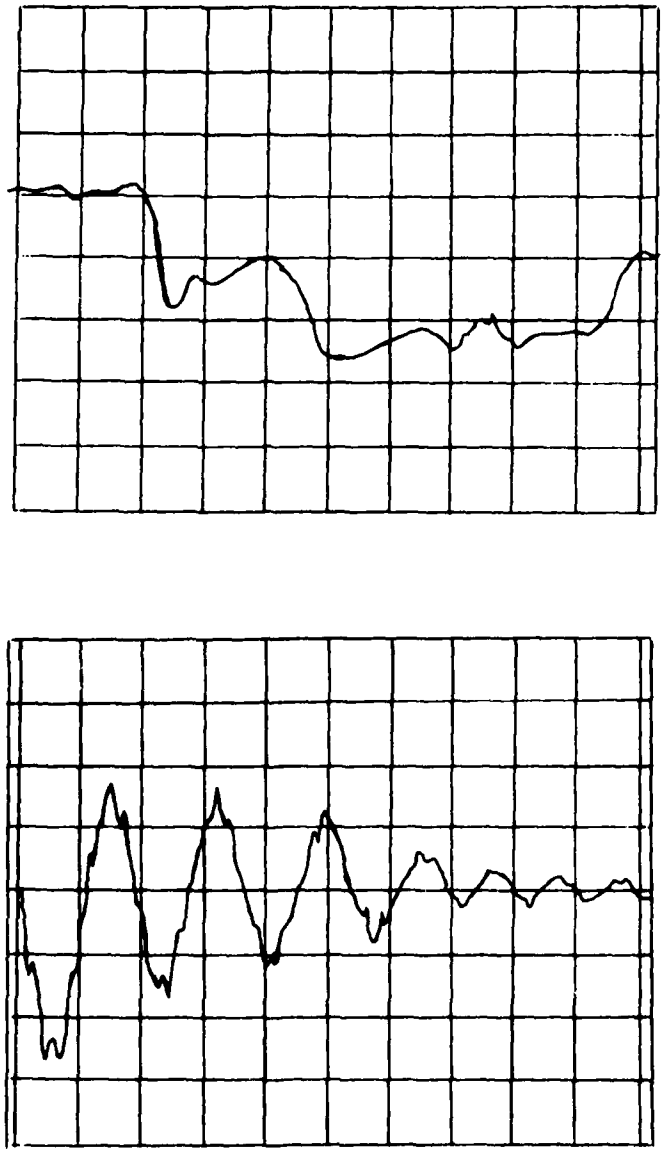

Figure 9. Output Waveform for $Z_2 = (1/4.30)\ Z_1$ Line-Pair. (a) 5 ns/div; 200 mv/div. (b) 50 ns/div; 200 mv/div.

V_0 with transfer of 100% of the energy stored in the transmission line to the load. Figure 8(a) shows the sensor output for a line pair with $Z_2 = 3Z_1$, i.e., with the switch located in the low impedance line. Again it is seen that the basic nature of the waveform is preserved through several transits of the line pair. Figure 8(b) shows the same waveform on a compressed time scale. The exponential decaying envelope is again a consequence of the sort time constant in the sensor circuit. The signals were generally too small to permit passive integration at either the sensor locations or at the oscilloscope.

Figure 9 shows the output for the 1.83 M line pair with $Z_2/Z_1 = 4.30$. As suggested earlier one sees that the repetitive transits of the line smooth out somewhat the voltage steps providing a sine-like repeating waveform which may offer some advantage for operation in a recirculating mode.

The strip-line experiments described in this section were conducted while a full-scale model in a folded coaxial-cavity geometry was being built. In the following section, measurements with the coaxial cavity are described.

C. Folded Coaxial-Cavity Experiments

A line drawing of the cavity is shown in Fig. 10. The intermediate and outer tubes were fabricated from rolled aluminum plate 4.8 mm thick. The dimensions of the cylinders are as follows: outer cylinder, I.D. = 97 cm; intermediate cylinder, I.D.=54 cm; drift tube, I.D. = 10 cm. The length of the cavity was chosen to give a double transit time, $2T\ell$, of approximately 20 nsec. The intermediate tube was supported in position by either polyethylene legs (2-line cavity) or styrofoam panels (3-line system).

The cavity was normally switched with five avalanche transistors in one of two arrangements, axial or radial, as indicated in Fig. 16. Switching was controlled by a fast pulser which triggered a pulse generator with five outputs, each with an independently adjustable delay. Current probes in the base of the avalanche transistor permitted synchronization of the switch firings to approximately 0.25 nsec.

The switching circuit was sometimes as simple as "hook-up wire" or metal ribbons connecting the intermediate cylinder to the high voltage supply and to the transistor switches mounted on the end plate external to the cavity. More often the switches were laid out on circuit board material in an attempt to reduce circuit (switch) inductance.

Normally the sensor was an annular capacitive pickup located in the output transmission line approximately 10-12 cm from the acceleration gap. The capacitor was formed by the outer surface of the drift tube (Fig. 10) and a 2.54 cm wide metal ring (or clamp) insulated from the drift tube by a 127 μm thick mylar foil. Initial results obtained with small gap spacings, of 5 cm, are shown in Fig. 11. The RC time constant for the sensor capacitance and the 50 ohm transmission line is short relative to the pulse duration of interest which results in a modification of the output waveforms switch. This figure also illustrates the effect of limited changes in inductance; thus, changing the number of switches bound to 5 can have a marked effect in the risetime and duration of the "top" of the pulse at the gap.

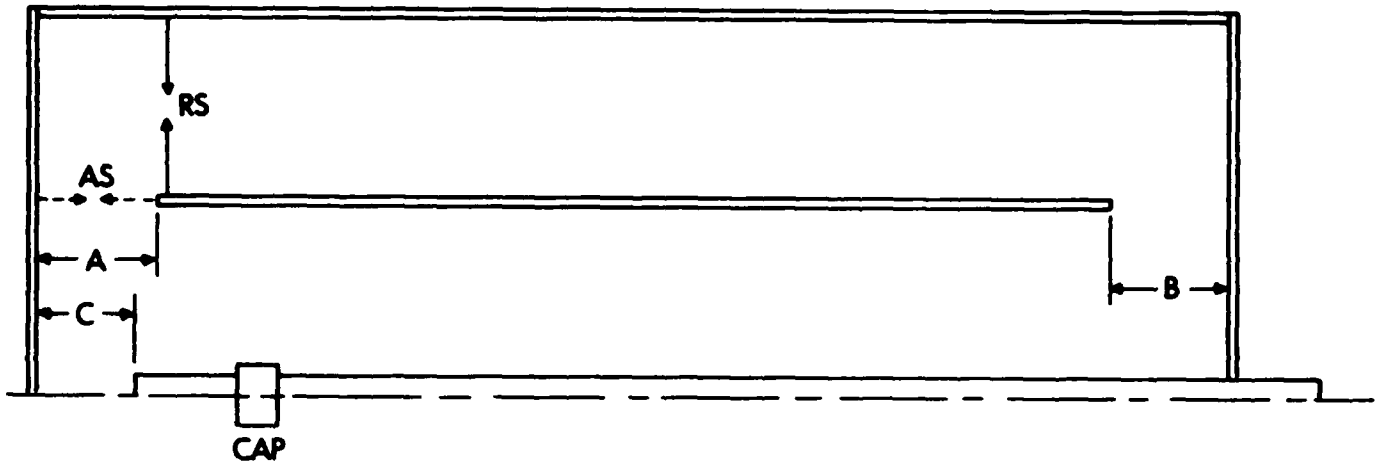

Figure 10. Line Drawing of Two-Line Folded Coaxial-Cavity. Switching of the inner cylinder to the outer (ground) is accomplished by either an array of Radial Switches, RS, or an array of Axial Switches, AS. CAP denotes the Sensor Capacitor and C represents the acceleration gap.

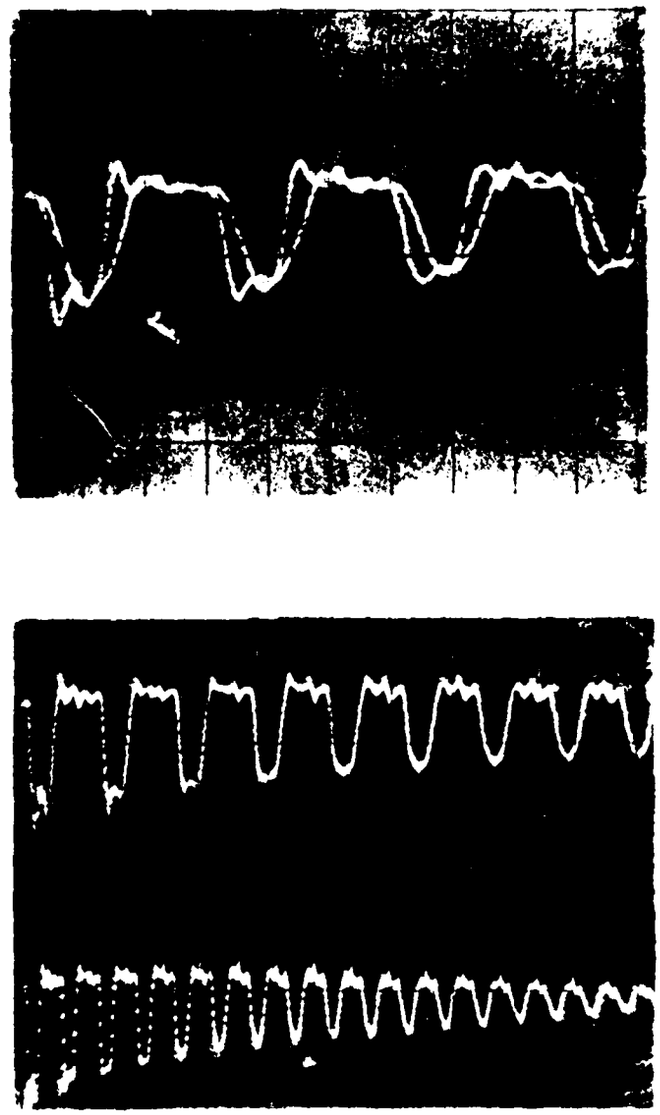

Figure 11. Output Waveform for $Z_2 = 3Z_1$, Folded-Coax Cavity. (a) 20 ns/div; 100 mv/div (one-switch and five-switch configurations). (b) Top trace calibration: 50 ns/div; bottom trace calibration 100 ns/div.

Two other methods of looking at the output voltage waveform were used. A disc-shaped capacitor (with 255 μm plate spacing and mylar dielectric) was used by removing the drift-tube extension and terminating the accelerator gap at the end plate of the tube. Results are given in Fig. 12 for accelerator gap and line junction spacings of 10.2 cm each. Additionally, signals were taken from a resistive divider connected across the acceleration gap. In this arrangement one end of a copper sulfate resistor is connected to ground at the end plate of the cavity (see Fig. 10) while the other end is positioned just inside the drift tube by a spacer which insulates it from the drift tube. This end of the resistor is connected to a 50 Ω carbon resistor which is in turn connected to the drift tube wall. Observations were made for copper sulfate resistance values of approximately 280 Ω and 3150 Ω, the latter open circuit conditions for our 100 Ω line. Simultaneous observation of the sensor signal in line 2 (Fig. 10) and signals from either the disc capacitor or the resistive divider established that the open circuit waveform at the gap was well represented by the capacitor pickoff in line 2. Because this e-field (or E) sensor perturbs the cavity waveform less than any of the other devices, most of the studies were conducted using this method of recording the data.

When an axial switch array is used, in effect reducing the gap at A to zero, the lines ℓ_1 and ℓ_2 are most readily equalized by reducing the acceleration gap to effectively zero. With these artifically small spacings one gets an upper limit to waveform integrity for operation in a potential recirculation mode. In Fig. 13 are shown four waveforms for an axial switch assembly with the gap at C equal to 10.2 cm and a 0.3 cm gap at B. The deterioration in waveform is due largely to the discontinuity at the junction between lines 1 and 2 because the other spacings are effectively zero. In Fig. 14 the output for a more realistic discontinuity spacing is shown. For Fig. 14, the gaps at B and C were 25.4 cm (gap A was approximately zero). Although considerable "ringing" is evident, the basic characteristics of the $Z_1/Z_2 = 1{:}3$ configuration are evident for several cycles. Figure 14(c) illustrates the effects, over a limited range, of switch inductance on the output voltage. Figures 14(a) and (b) were obtained with five symmetrically placed avalanche transistor switches at two different oscilloscope time-base settings, 20 ns/div and 50 ns/div, respectively. Figure 14(c) shows five traces corresponding to 1, 2, 3, 4, and 5 switches. The longer risetimes and shifted "crossover times" on the voltage axis correspond to the fewest switches. Waveforms comparable to those of Figs. 13 and 14 are obtained for a reasonable range of parameters. Numerous kinds of field shapers, e.g., conical inserts to eliminate the corner at C and other locations were tried for this and other configurations without any apparent large effects.

III. EXPERIMENTAL (THREE-LINE SYSTEMS)

Closed form analytical solutions for the accelerating waveform have been obtained for ideal, lossless, three-line arrangements switched by ideal switches. Figure 15 shows the schematic representation of the three-line system with equal line lengths. One advantage of such an arrangement is that it permits the switches to be placed in a region of lower electric field than is the case for the two-line systems.

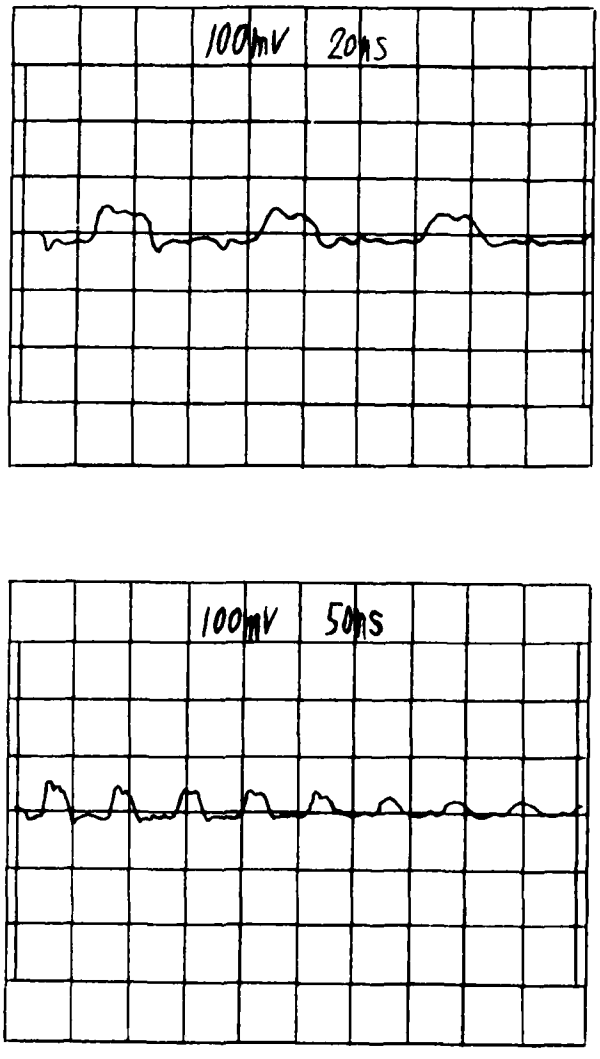

Figure 12. Output Waveform Taken With Disc Capacitor at End Plate of Folded-Coax Cavity. (a) 20 ns/div. (b) 50 ns/div.

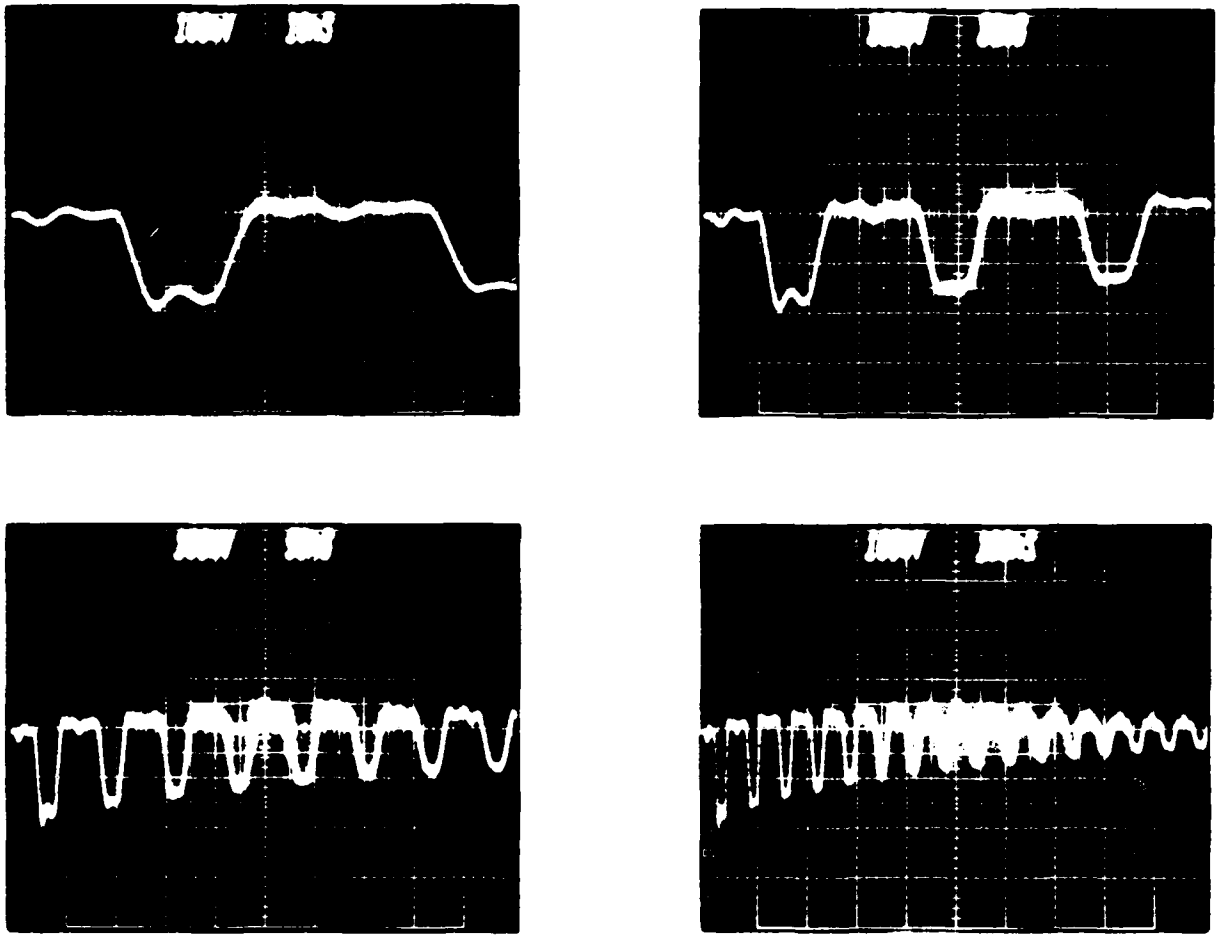

Figure 13. Sample Open-Circuit Waveform for Folded-Coaxial Cavity, a 2-Line System with $Z_2/Z_1 = 3$.

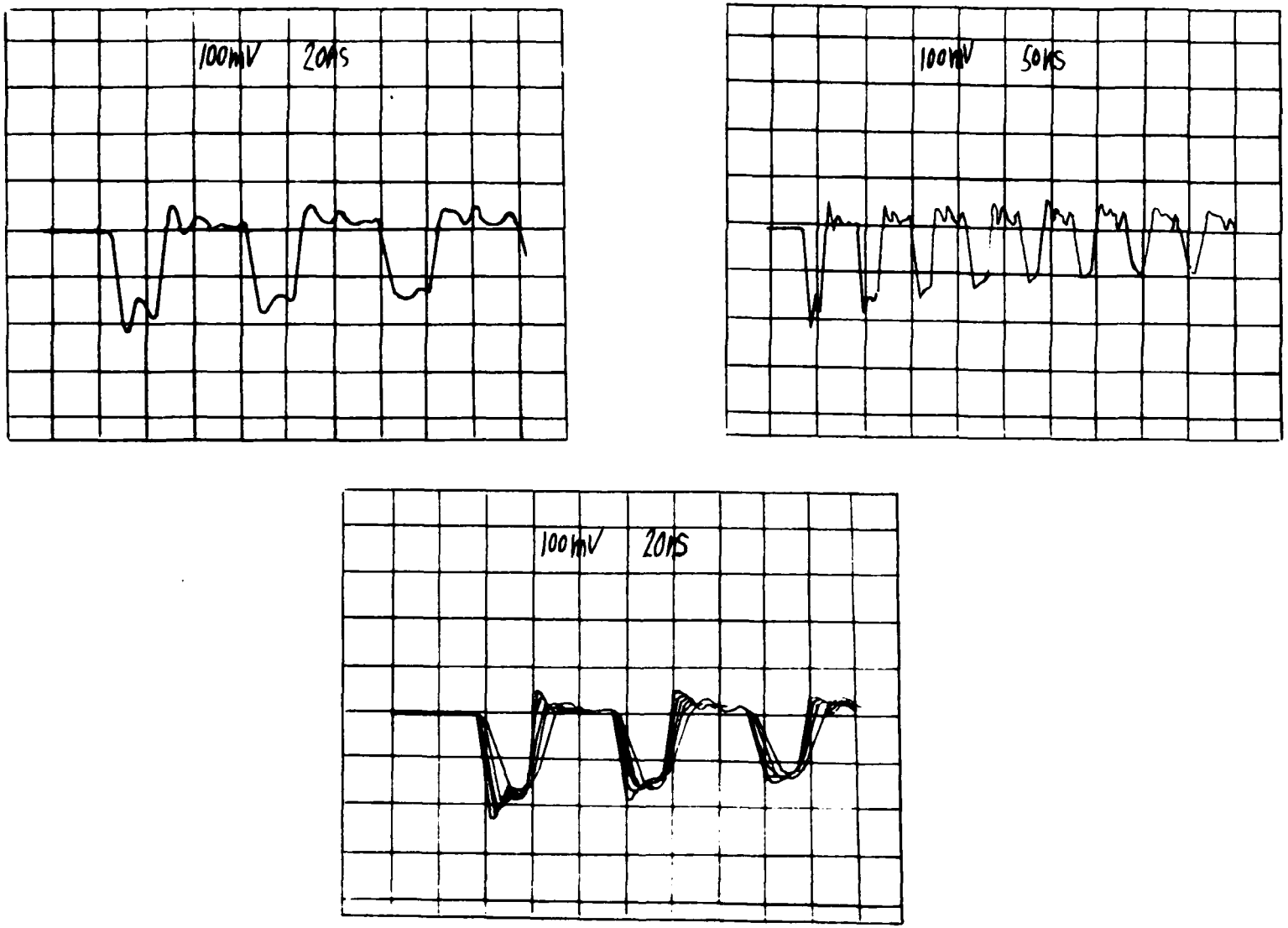

Figure 14. Output Waveforms for Folded Coaxial Cavity Geometries. (a) 20 ns/div. (b) 50 ns/div. (c) 20 ns/div. Waveforms for 1, 2, 3, 4, and 5 switches.

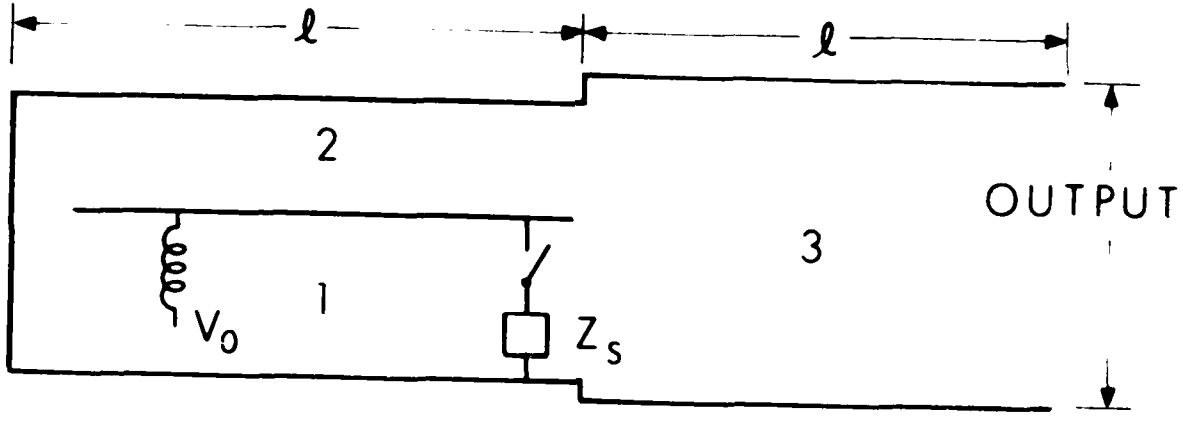

Figure 15. Schematic of the Three-Line System. V_0 is the charge voltage and Z_s is the impedance of the switch, assumed zero for the analysis summarized in this section.

In the prior analysis, it was shown that a set of line impedance ratios exists for which a nominal 100% efficiency is attained and some of the ratios afford voltage gain. Some ratios also give rise to a repeating open-circuit gap voltage which might be useful in an efficient recirculating beam accelerator. Recently it has been shown[18] that for certain impedance ratios it is possible to transfer energy with 100% nominal efficiency to a beam which is recirculated through the cavity. Preliminary discussions of the analysis of three-line arrangements may be found in References 11, 12, and 19 as well as in a paper by Ian Smith.[13] A more detailed account is to be published.[18]

The open circuit (OC) voltage for the ideal line is a sequence of pulses of width $2T\ell$, and the kth pulse is given by

$$V^{(k)} = \frac{V_0 \tau_{23}}{1 + \cos\theta} (\cos k\pi + \cos (k + 1)\theta) \tag{3}$$

where $\cos\theta = (1 - \rho)/2$ (4)

$$\rho = \rho_{12} + \rho_{23} + \rho_{12}\rho_{23} = \tau_{12}\tau_{23} - 1 \tag{5}$$

and ρ is given in terms of the usual reflection and transmission coefficients

$$\rho_{ij} = \frac{Z_j - Z_i}{Z_j + Z_i} \quad ; \quad \tau_{ij} = (1 + \rho_{ij}) \quad . \tag{6}$$

The OC waveform is repetitive when θ is a rational fraction of π or

$$\theta = \frac{p}{q}\pi \quad ; \; p < q \text{ are integers.} \tag{7}$$

Some examples of the open-circuit voltage predicted by Equation (3) are shown in Fig. 16.

The model tests for the three-line systems were conducted in a similar fashion to those discussed previously; i.e., experiments were conducted with cables and in a parallel-plate geometry while additional tubes were being fabricated to convert the one metre diameter folded coaxial-cavity to a three-line arrangement.

A. Cable Experiments

Simulation of the three-line systems with coaxial cables is not as straightforward as for the two-line systems. Two arrangements which do simulate the $Z_1:Z_2:Z_3::1:1:1$ system are shown in Fig. 17. The requirement to cross connect shield and center conductors not only introduces additional unwanted lengths of line but also requires that part of the line be an open geometry, i.e., not coaxial.

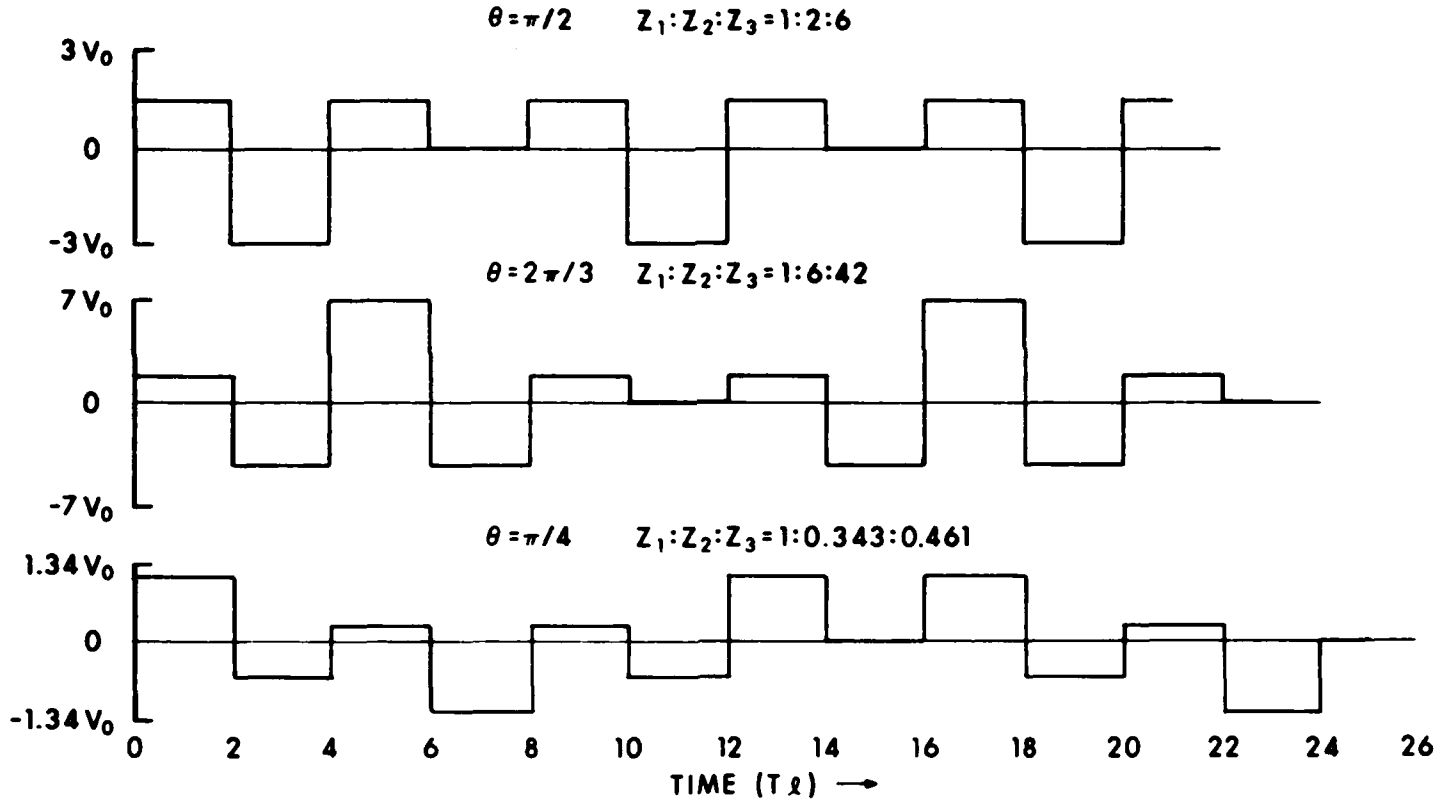

Figure 16. Predicted Open-Circuit Waveform for Selected Impedance Ratios in Three-Line Configurations.

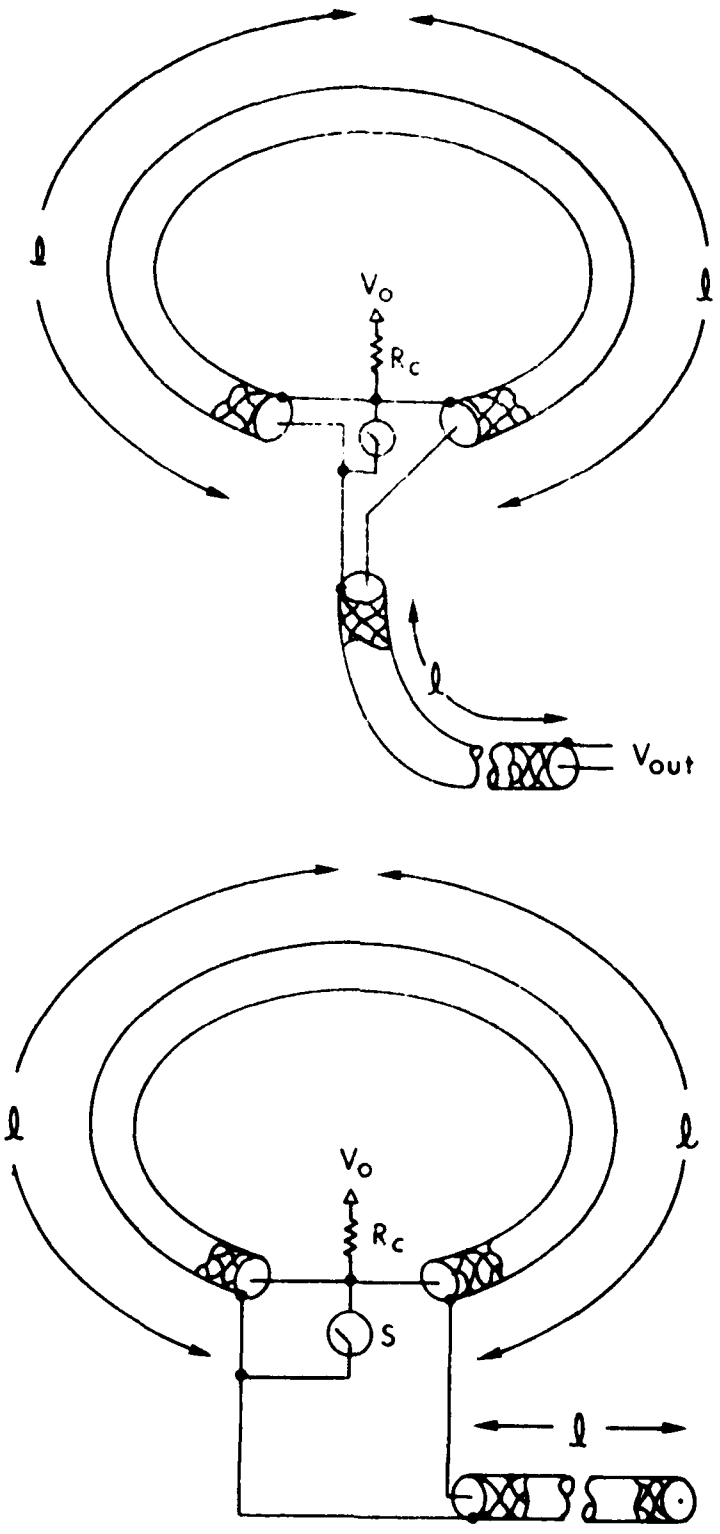

Figure 17. Two Methods of Simulating Three-Line Systems With Coaxial Cables (1:1:1 Systems).

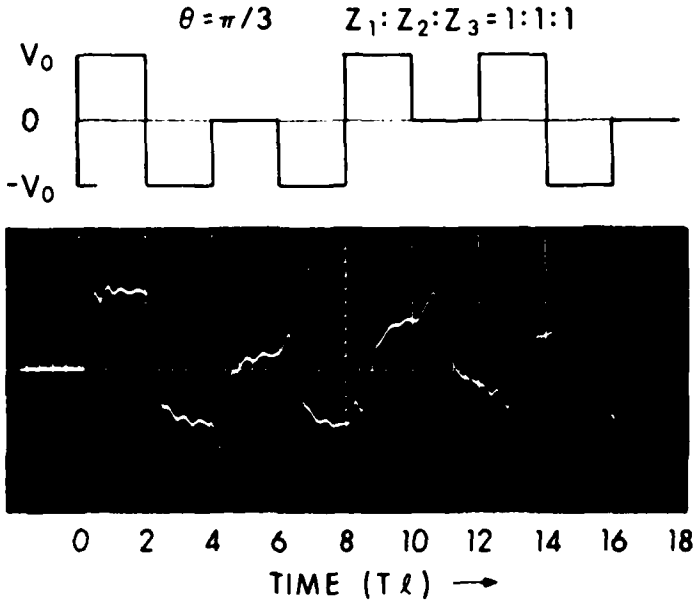

Figure 18. Predicted and Observed Waveforms for $Z_1:Z_2:Z_3$ = 1:1:1.

Figure 18 shows the predicted and observed output waveforms from the coaxial array ($Z_1 = Z_2 - Z_3 = 50\ \Omega$). Equation (3) implies that in contrast to the two-line configurations it is not possible to have a waveform that rises to a peak in succession of pulse periods, $2T\ell$, for three-line systems. In the three-line case successive pulses must alternate in polarity. This later prediction seems to be born out by the results displayed in Fig. 18; however, a better quality waveform is necessary in order to demonstrate convincingly the validity of Eq. (3). For that a different geometry is required.

B. Parallel-Plate Transmission Line Experiments

Circuit-board material was used to construct a three-line system similar to the two-line system described previously with the same sensor capacitor located near the output end of Line 3. Output waveforms from a $Z_1:Z_2:Z_3 = 1:1:2$ line are shown in Fig. 19. Although not repetitive, this configuration illustrates a feature of all the strip-line data for three-line systems; a glitch was observed at approximately $6T\ell$ into the pulse, i.e., the time required for a pulse to travel from the output terminal to the switch and return.

A more interesting configuration, perhaps the most important one from a practical standpoint, is the $Z_1:Z_2:Z_3 = 1:2:6$ system shown in Fig. 20. This configuration produces a repetitive OC waveform and is capable of transferring 100% of the energy stored in the cavity to a resistive beam load. Note the similarity of the occurrence of the glitch in this waveform with that observed in Fig. 19. The switch was moved from Line 1 to Line 2 which converted the system to a 2:1:6 configuration with results as shown in Fig. 21. The amplitude of the glitch is reduced somewhat; but by the second pulse, at $12T\ell$, the effect is again significant.

Because the effect appeared to be associated with current reversals in the switch, we next tried a mechanical switch. Some results are shown in Fig. 22 for a 1:2:6 line mechanically switched. Although the switch works rather well and leads to a reasonable output waveform, a troublesome glitch which severely distorts the waveform between $6T\ell$ and $8T\ell$ is evident.

Inability to eliminate this glitch, or to fully understand it, led us to drop the strip-line experiments to await construction of the intermediate tubes required to convert the folded-coax unit to a three-line system. Subsequent experiments with the folded-coax, described in the following sections, showed that similar effects or glitches could be produced by unequal line lengths under certain conditions. Thus it is possible that the glitches in the parallel plate experiments are a consequence of unequal line lengths resulting from the "open geometry" of the lines, e.g., they couple in some difficult-to-determine manner to the surroundings. But this is conjecture and was not proved in the present experiments.

In a final attempt to improve the output waveforms for this geometry, conducting shields, i.e., extensions of the parallel plates, were used in the vicinity of the junction between line 3 and lines 1 and 2 in an attempt to reduce any cross talk or coupling between line 3 and the other lines. No noticeable difference was observed. At this point the parallel plate experiments were abandoned in favor of the folded-coax geometry.

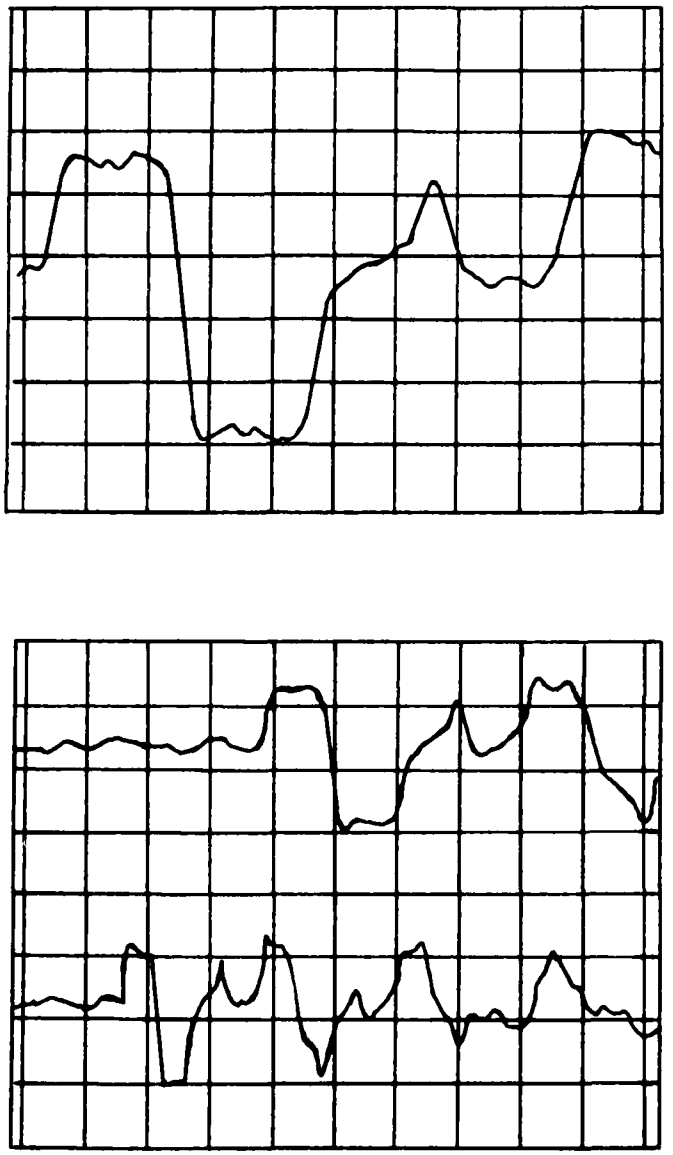

Figure 19. Open-Circuit Voltage for $Z_1:Z_2:Z_3$ = 1:1:2. Parallel-Plate Transmission line. (a) 5 ns/div. (b) 10 ns/div. (c) 20 ns/div.

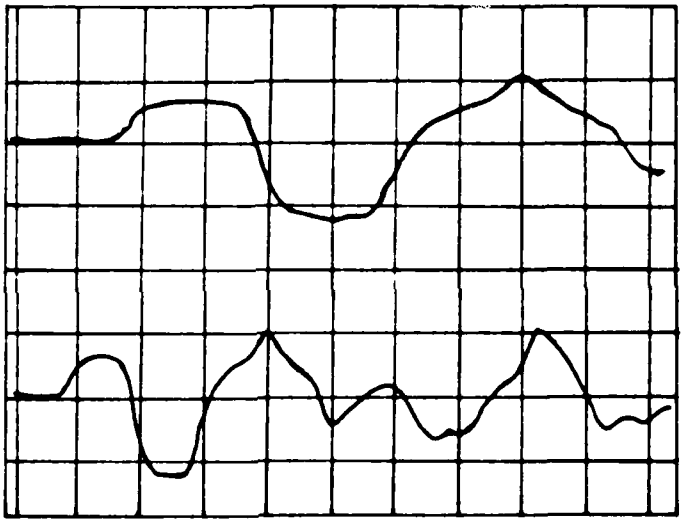

Figure 20. Output of $Z_1:Z_2:Z_3 = 1:2:6$ Parallel-Plate Transmission Line. (a) 10 ns/div. (b) 20 ns/div.

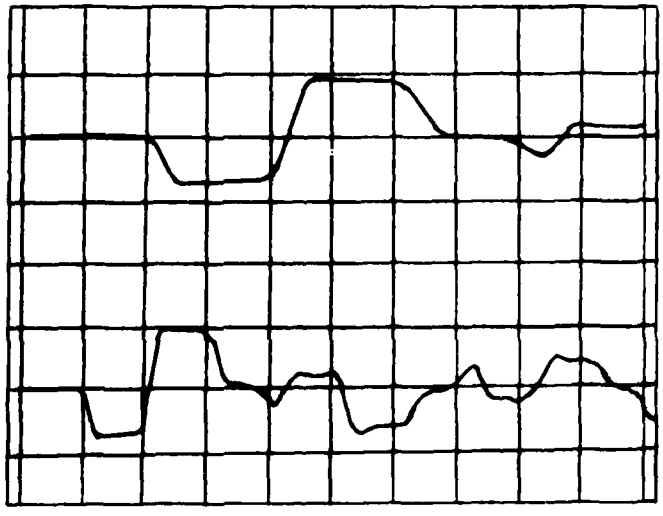

Figure 21. Open-Circuit Voltage From $Z_1:Z_2:Z_3 = 2:1:6$. Parallel-plate transmission line. (a) 10 ns/div. (b) 20 ns/div.

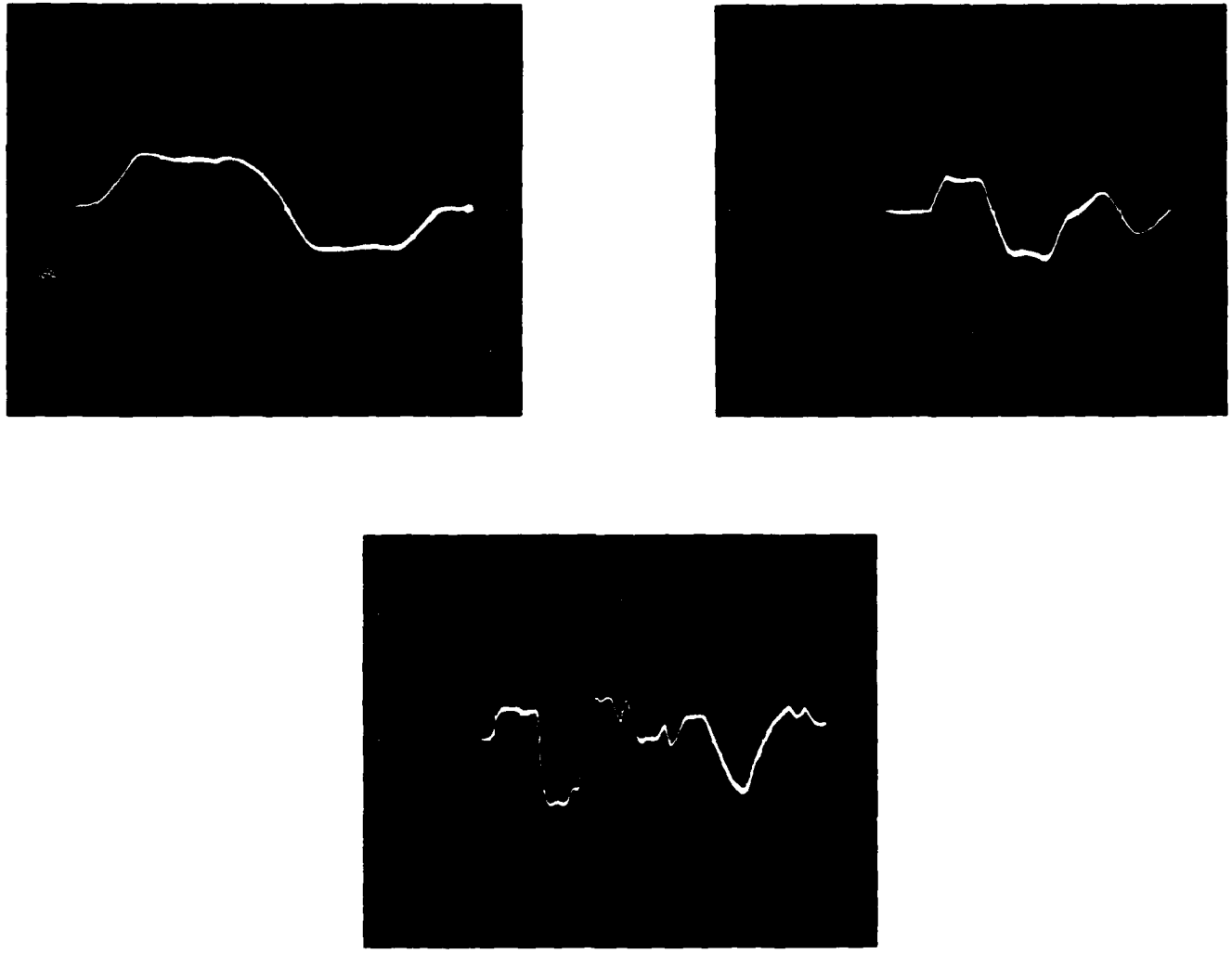

Figure 22. Open-Circuit Voltage From $Z_1:Z_2:Z_3$ = 1:2:6, Parallel-Plate Line Mechanically Switched. (a) 2 ns/small div; 100 mv/div. (b) 5 ns/small div. (c) 10 ns/large div.

C. Folded Coaxial-Cavity Experiments

Two new intermediate tubes were fabricated in order to convert the coax assembly to the three-line system (1:2:6) shown in Fig. 23. The dimensions (I.D.S.) of the intermediate cylinder are 75 cm and 45 cm, respectively. Initially a radial switch array located 30.5 cm from the end plate (gap A of Fig. 23) was used with all gaps (A, B, C, and D) equal to 30.5 cm, corresponding to differences of around 6% in line lengths. The observed waveforms showed a glitch similar to that observed in the parallel-plate experiments. The similarity of the glitch at time $\tau = 6T\ell$ to that observed many times in the strip-line experiments was apparent.

To realize approximately equal line lengths, an axially mounted switch was used to connect the shorter intermediate tube to the cavity end plate and the acceleration gap, D in Fig. 23, was reduced to 15.2 cm. The gaps at B and C were set to 2.54 cm. The results are shown in Fig. 24. These data demonstrate convincingly the essential correctness of the E/T analysis and the repetitive nature of the open circuit waveform for the $Z_1:Z_2:Z_3 = 1:2:6$ system. Some indication of the effect of inductance on the output is shown in Fig. 25 which shows a superimposition of waveforms for 1, 2, 3, 4 and 5 switches, respectively.

Many different configurations were tried during the course of the experiments. Representative of the better results obtained with realistic gap spacings are those shown in Fig. 26. Although the detailed features of the waveform in the region of time between acceleration pulses are washed out after the initial pulse and some "ringing" is evident, the first three or four acceleration pulses are reasonably well reproduced. These results were obtained with an axial switch array and the following gap spacings: Gap A ≃ 0, Gap B = 12.7 cm, Gap C = Gap D = 30.5 cm.

As was the case with the two-line system, conical shapers were tried at the line junctions with no significant effects on the output. A possible exception occurred when radially arrayed switches were employed. In this case a deflector attached to the shorter intermediate tube (Fig. 14), which efficiently reduced the impedance discontinuity at the switch end of the cavity, appeared to improve slightly the output waveform; but the effect was not dramatic.

IV. SUMMARY AND CONCLUSIONS

It is useful to reiterate the goals of the present experiments. They are as follows: (1) to verify previous analyses of both two- and three-line transmission-line configurations which appear promising for electron acceleration and (2) to study the effects of the discontinuities at the line junctions on the open circuit waveform, particularly for line configurations which result in repetitive open-circuit waveforms.

The analysis by Eccleshall and Temperley of energy transfer for pairs of asymmetric, charged, transmission lines and the more recent analysis by Eccleshall of the analogous problem in three-line systems were verified in a variety of simulation experiments.

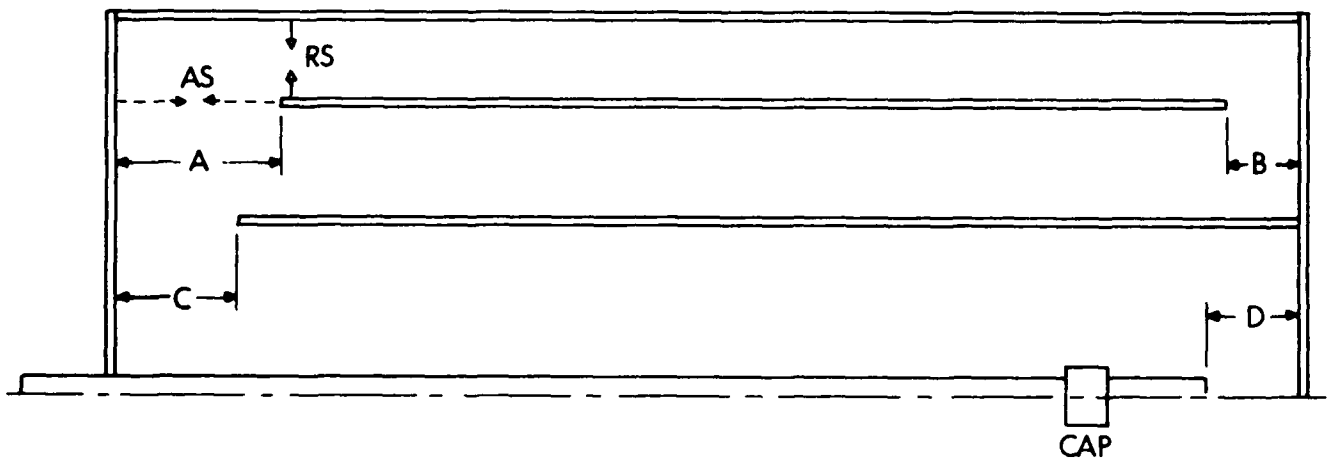

Figure 23. Line Drawing of Three-Line, Folded Coaxial-Cavity. See caption for Figure 10.

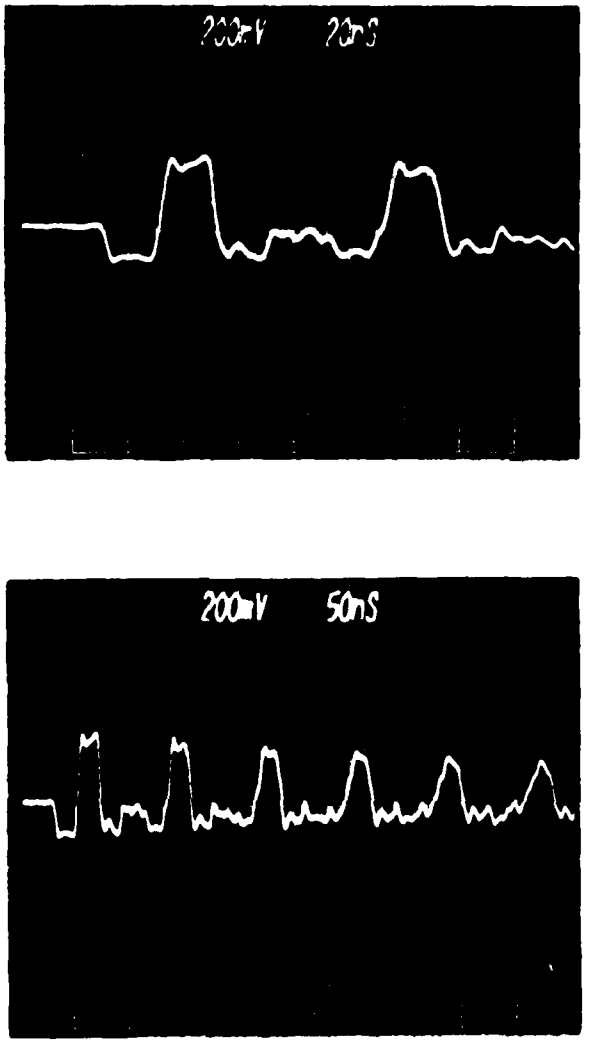

Figure 24. Open-Circuit Voltage From Three-Line Folded Coaxial-Cavity for Small Gap-Spacings.

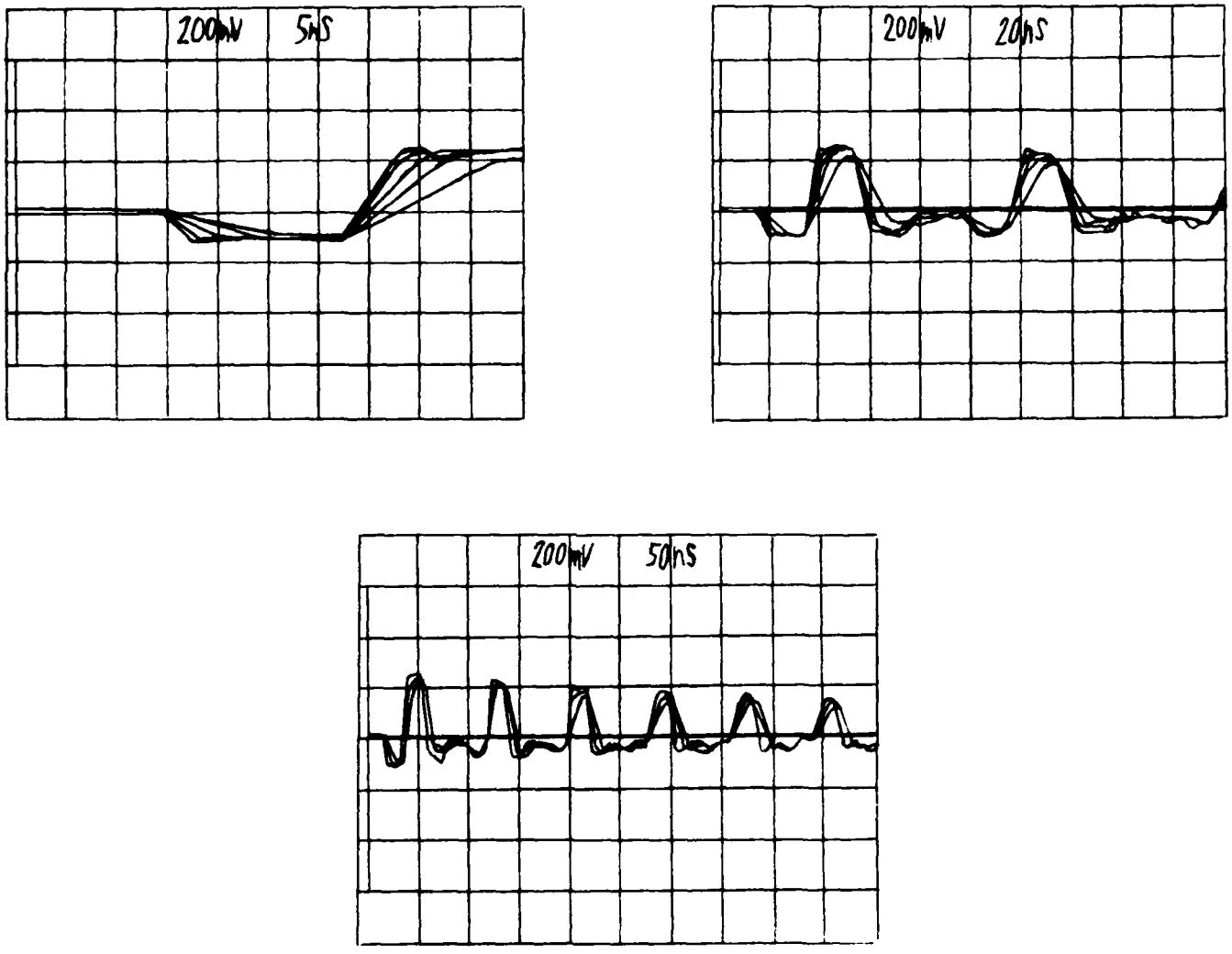

Figure 25. Output of Folded Coaxial-Cavity for 1,2,3,4 and 5 Switches.

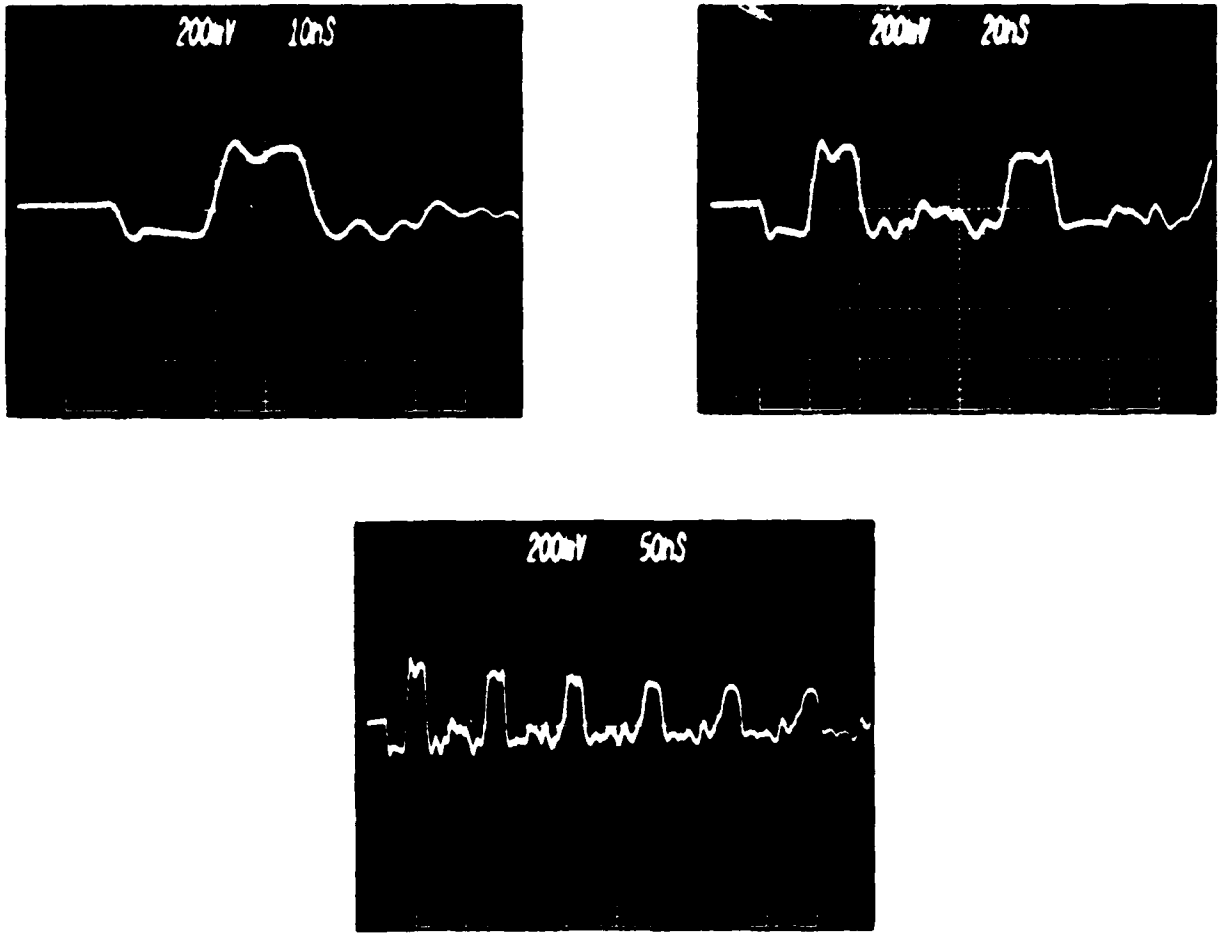

Figure 26. Open-Circuit Output of Folded Coaxial Cavity for Realistic Gap Spacings.

The effects of the line-junction discontinuities on the OC waveform are, in principle, amenable to analysis; however, this approach could become cumbersome if one is interested in long times and many wave traversals of the cavity, as for example in a recirculation scheme. Therefore, low-voltage model studies were carried out to study these effects.

In order to isolate the effects of the discontinuities from other factors the experimental model was made as ideal as possible. This, of course, sidesteps many of the more important issues which determine the potential usefulness of these configurations for particle acceleration, such as finite impedance switches; spark gaps with both inductive and resistive phases; voltage standoff and field-grading requirements; gap design and limitations imposed by mechanical considerations. Nonetheless, it is important to know, as these studies show, that the distortions introduced by the line discontinuities are not unacceptable for several complete cycles in the cavity geometries envisioned for recirculation accelerators. Finally, we note that high voltage tests are now underway at the Sandia National Laboratory[20] with full-scale, liquid-dielectric loaded, cavities of the type considered by Eccleshall and Temperley and by Smith.

ACKNOWLEDGEMENTS

The author wishes to acknowledge the advice and encouragement received from Dr. D. Eccleshall throughout the course of the work reported herein.

Drs. Alan Bromborski and Al Kehs of the Harry Diamond Laboratories furnished valuable advice and provided the avalanche transistor switches and triggering circuitry as well as some of the strip-line models used in the experiments.

Dr. G.M. Thomson contributed to the design and construction of the two-line cavity and Phil Yunker assisted in the data-taking for the strip lines. Finally, Joe Correri fabricated structures and switches and assisted in obtaining most of the experimental data. These contributions are gratefully acknowledged.

[20] *K.R. Prestwich and W. Tucker, private communication.*

REFERENCES

1. James E. Leiss, "Induction Linear Accelerators and Their Applications," IEEE Trans. Nucl. Sci. NS-26, No. 3, 3870-76, 1979.

2. H. Christofilos, R.E. Hester, W.A.S. Lamb, D.D. Reagan, W.A. Sherwood, and R.E. Wright, "High Current Linear Induction Accelerator for Electrons," Rev. Sci. Instr. 35, 886-890, 1964.

3. Ross E. Hester, Donald G. Bubp, John C. Clark, Alfred W. Chesterman, Edward G. Cook, Warren L. Dexter, Thomas J. Fessenden, Louis L. Reginato, Ted T. Yokota, and Andris A. Faltens, "The Experimental Test Accelerator (ETA)," IEEE Trans. Nucl. Sci. NS-26, No. 3, 4180-82, 1979.

4. R.J. Briggs, D.L. Birx, G.J. Caporaso, T.J. Fessenden, R.E. Hester, R. Melendes, V.K. Neil, A.C. Paul, and K.W. Struve, "Beam Dynamics in the ETA and ATA 10 kA Linear Induction Accelerators: Observations and Issues," IEEE Trans. on Nucl. Sci. NS-28, No. 3, 3360-64, 1981. See also Physics Today, February 1982, p. 20.

5. R. Avery, G. Behrsing, W.W. Chupp, A. Faltens, E.C. Hartwig, H.P. Hernandez, C. MacDonald, J.R. Meneghetti, R.J. Nemetz, W. Popenuck, W. Salsig and Vanecek, "The ERA 4 MeV Injector," IEEE Trans. Nucl Sci. NS-18, 479-483, 1971.

6. J.E. Leiss, "Modern Electron Linacs and New User Needs," Proc. 1972 Proton Linac Conference, Los Alamos, LA-5115, UC-28 (1972).

7. A.J. Anatskii, O.S. Boedanev, P.V. Bukaev, Yu P. Vakhrushin, I.F. Malyshev, G.A. Nalivaika, A.I. Pavlov, V.A. Suslov, and E.P. Khalchitskii, "Linear Induction Accelerator," Sov. At. En. 21, 1134-1140, 1966.

8. A.I. Pavlovskii, V.S. Bosamykin, G.D. Kuleshov, A.I. Gerasimov, V.A. Tananakin, and A.P. Kumentev, "Multielement Accelerator Based on Radial Lines," Sov. Phys. Dokl, 20, 441-443, 1975.

9. Radlac Radial Line Accelerator Progress Report, October 1977 through 1978, Sandia National Laboratory Report, SAND-2129, Jan 1980.

10. R.B. Miller, J.W. Poukey, B.G. Epstein, S.C. Shope, T.C. Genoni, M. Franz, B.B. Godrey, R.J. Adler and A. Mondelli, "Beam Transport Issues in High Current Linear Accelerators," IEEE Trans. Nucl. Sci. NS-28, No. 3, 3343-3345, 1981.

11. D. Eccleshall and J.K. Temperley, "Transfer of Energy from Charged Transmission Lines with Application to Pulsed High-Current Accelerators," J. Appl. Phys. 49(7), 3649-3655, 1978. See also J.K. Temperley and D. Eccleshall, "Analysis of Transmission-Line Accelerator Concepts," USA ARRADCOM Technical Report, ARBRL-TR-02067, May 1978 (AD A056364), and J. K. Temperley, "Analysis of Coupling Region in Transmission-Line Accelerators," USA ARRADCOM Technical Report, ARBRL-TR-02120, Nov 1978 (AD A063463).

REFERENCES

12. D. Eccleshall, J.K. Temperley, and C.E. Hollandsworth, "Charged, Internally Switched Transmission Line Configurations for Electron Acceleration," IEEE Trans. Nucl. Sci. NS-26, No. 3, 4245 (1979).

13. Ian D. Smith, "Linear Induction Accelerators Made from Pulse-Line Cavities with External Pulse Injection," Rev. Sci. Instrum. 50, 714, 1979.

14. J.R. Whinnery and H.W. Jamieson, "Equivalent Circuits for Discontinuities in Transmission Lines," Proc. IRE 32, 98-115, 1944.

15. J.R. Whinnery, H.W. Jamieson and T. E. Robbins, "Coaxial-Line Discontinuities," Proc. IRE 32, 695-704, 1944.

16. J.R. Whinnery and D.C. Stinson, "Radial Line Discontinuity," Proc. IRE 43, 46-51, (1955).

17. David B. Sidel, "Discontinuity Effects on Radial Cavity Transmission Lines," Sandia Laboratories Report SAND-79-1056, April 1979.

18. D. Eccleshall, private communication.

19. Donald Eccleshall and C.E. Hollandsworth, "Transmission-Line Cavity Linear-Induction Accelerator," IEEE Trans. Nucl. Sci. NS-28, No. 3, 3386 (1981).

20. K.R. Prestwich and W. Tucker, private communication.

DISTRIBUTION LIST

No. of Copies	Organization
12	Administrator Defense Technical Info Center ATTN: DTIC-DDA Cameron Station Alexandria, VA 22314
1	Commander US Army Materiel Development & Readiness Command ATTN: DRCDMD-ST 5001 Eisenhower Avenue Alexandria, VA 22333
1	Commander Armament R&D Center US Army AMCCOM ATTN: DRSMC-TDC(D) Dover, NJ 07801
1	Commander US Army Armament, Munitions and Chemical Command ATTN: DRSMC-LEP-L(R) Rock Island, IL 61299
1	Director Benet Weapons Laboratory Armament R&D Center US Army AMCCOM ATTN: DRSMC-LCB-TL(D) Watervliet, NY 12189
1	Commander US Army Aviation Research & Development Command ATTN: DRDAV-E 4300 Goodfellow Blvd St. Louis, MO 63120
1	Director US Army Air Mobility Research & Development Laboratory Ames Research Center Moffett Field, CA 94035
2	Commander Armament R&D Center US Army AMCCOM ATTN: DRSMC-TSS(D) Dover, NJ 07801
1	Commander US Army Communications Research & Development Command ATTN: DRSEL-ATDD Fort Monmouth, NJ 07703
1	Commander US Army Electronics Research & Development Command Technical Support Activity ATTN: DELSD-L Fort Monmouth, NJ 07703
1	Commander US Army Missile Command ATTN: DRSMI-R Redstone Arsenal, AL 35898
1	Commander US Army Missile Command ATTN: DRSMI-YDL Redstone Arsenal, AL 35898
1	Commander US Army Tank Automotive Command ATTN: DRSTA-TSL Warren, MI 48090
1	Director US Army TRADOC Systems Analysis Activity ATTN: ATAA-SL White Sands Missile Range, NM 88002
2	Commandant US Army Infantry School ATTN: ATSH-CD-CSO-OR Fort Benning, GA 31905
1	DARPA ATTN: LTC R. Gullickson 1400 Wilson Blvd Arlington, VA 22209
1	Commander US Army Missile Command ATTN: Dr. T.G. Roberts Redstone Arsenal, AL 35898

DISTRIBUTION LIST

No. of Copies	Organization
3	Commander US Army Harry Diamond Labs ATTN: DELHD-RBC, Dr. Bromborsky Dr. A. Kehs DELHD-PP, S. Graybeal 2800 Powder Mill RD Adelphi, MD 20783
1	Commander US Army TRADOC ATTN: ATDO-ZT Dr. Marvin Pastel Fort Monroe, VA 23651
1	Commander US Army Foreign Science & Technology Center ATTN: Dr. Thomas Caldwell 220 Seventh Street, NE Charlottesville, VA 22901
1	HQDA (DAMA-ARZ-A) Washington, DC 20310
1	HQDA (DAMA-CSM-CS) Washington, DC 20310
2	Commander US Army Research Office ATTN: Dr. Herman Robl Dr. Randy Jones PO Box 12211 Research Triangle Park, NC 27709
2	Director US Army BMD Advanced Technology Center ATTN: ATC-D, Mr. Milt Howie PO Box 1500 Huntsville, AL 35807
1	Office of Naval Research ATTN: Dr. C.W. Robertson 800 N. Quincy Street Arlington, VA 22217

No. of Copies	Organization
1	Commander Naval Surface Weapons Center ATTN: Code WR-401, Dr C.M. Huddleston Silver Spring, MD 20910
3	Commander Naval Research Laboratory ATTN: Code 77002, Dr. M.A. Sprangle Mr. J. Golden Dr. Kapetanakos Washington, DC 20375
1	AFWL/SUL Kirtland AFB, NM 87117
3	AFWL/NTYP ATTN: LTC J. Head Dr. David Straw Dr. W. Baker Kirtland AFB, NM 87117
1	AFWL (LTC Havey) Kirtland AFB, NM 87117
1	Director Los Alamos Scientific Laboratory ATTN: MS H818, Dr. Harald Dogliani P.O. Box 1663 Los Alamos, NM 87544
2	Director Lawrence Livermore Laboratory ATTN: L-306, Dr. R.J. Briggs L-306, Dr. T. Fessenden University of California PO Box 808 Livermore, CA 94550
3	Director Sandia National Laboratory Pulsed Power Directorate ATTN: R.B. Miller K. Prestwich W. Tucker Albuquerque, NM 87115

DISTRIBUTION LIST

No. of Copies	Organization
1	Department of Energy ATTN: Code ER-20.1, GTN, Mr. G.J. Peters Washington, DC 20545
1	Director National Bureau of Standards ATTN: Dr. M. Wilson Director, Center for Radiation Research Room 229, Bldg 245 Washington, DC 20234
1	Director ATTN: J.C. Nall PO Box 1925 Washington, DC 20505
1	Maxwell Laboratories, Inc. ATTN: Bill DeVoss 9244 Balboa Avenue San Diego, CA 92123
1	Battelle Columbus Laboratories ATTN: Dr. C.T. Walters Associate Manager, Physical Sciences Section 505 King Avenue Columbus, OH 43201
2	Physical Dynamics, Inc. ATTN: Dr. K. Brueckner Mr. John Shea PO Box 556 La Jolla, CA 92038
1	Rand Corporation ATTN: Dr. S. Kassel 2100 M Street, NW Washington, DC 20002
1	Science Applications, Inc. ATTN: Dr. R. Johnston 2680 Hanover Street Palo Alto, CA 94304
1	University of California Lawrence Berkeley Laboratory ATTN: Dr. Dennis Keefe Berkeley, CA 94720
1	Pulse Sciences, Inc. ATTN: I. Smith 14796 Wicks Blvd. San Leandro, CA 94577
1	Mission Research Corporation ATTN: Dr. Brendan Godfrey 1720 Randolph RD, SE Albuquerque, NM 87106
1	Science Applications, Inc. ATTN: Dr. A. Mondelli 1710 Goodridge Drive McLean, VA 22102
1	Department of Energy ATTN: Code C-404, Dr. Terry Godlove Washington, DC 20545
	Aberdeen Proving Ground
	Dir, USAMSAA ATTN: DRXSY-D DRXSY-MP, H. Cohen
	Cdr, USATECOM ATTN: DRSTE-TO-F
	Cdr, CRDC, AMCCOM ATTN: DRSMC-CLB-PA DRSMC-CLN DRSMC-CLJ-L

USER EVALUATION OF REPORT

Please take a few minutes to answer the questions below; tear out this sheet, fold as indicated, staple or tape closed, and place in the mail. Your comments will provide us with information for improving future reports.

1. BRL Report Number _____

2. Does this report satisfy a need? (Comment on purpose, related project, or other area of interest for which report will be used.)

_____

_____

_____

3. How, specifically, is the report being used? (Information source, design data or procedure, management procedure, source of ideas, etc.) _____

_____

_____

4. Has the information in this report led to any quantitative savings as far as man-hours/contract dollars saved, operating costs avoided, efficiencies achieved, etc.? If so, please elaborate.

_____

_____

5. General Comments (Indicate what you think should be changed to make this report and future reports of this type more responsive to your needs, more usable, improve readability, etc.) _____

_____

_____

_____

6. If you would like to be contacted by the personnel who prepared this report to raise specific questions or discuss the topic, please fill in the following information.

Name: _____

Telephone Number: _____

Organization Address: _____

_____

_____

FOLD HERE

Director
US Army Ballistic Research Laboratory
ATTN: DRSMC-BLA-S (A)
Aberdeen Proving Ground, MD 21005

NO POSTAGE
NECESSARY
IF MAILED
IN THE
UNITED STATES

OFFICIAL BUSINESS
PENALTY FOR PRIVATE USE $300

BUSINESS REPLY MAIL
FIRST CLASS PERMIT NO 12062 WASHINGTON, DC

POSTAGE WILL BE PAID BY DEPARTMENT OF THE ARMY

Director
US Army Ballistic Research Laboratory
ATTN: DRSMC-BLA-S (A)
Aberdeen Proving Ground, MD 21005

FOLD HERE